الجمهورية الجزائرية الديمقراطية الشعبية

PEOPLE'S DEMOCRATIC REPUBLIC OF ALGERIA

وزارة التعليم العالي والبحث العلمي

Ministry of Higher Education and Scientific Research

جـامـعـة عمّـــار ثـلـيـــجـــي بالأغـــواط

University of Amar Telidji - Laghouat

كلية التكنولوجيا

Faculty of Technology

قسم الالكتروتقني

Department of Electrical Engineering

MASTER Dissertation

Presented by:

RECHOUM Hakim / CHEMSEDDINE Mohamed Amine

Domain: Science and Technology

Field: Electrical Engineering

Option: Automation and Systems

Theme

Modeling & Intelligent Control of a Drilling-String System of Oil & Gas Wells

Jury members:

Full Name	**Grade**	**Quality**
Mr. BENMOUIZA Khalil	Prof.	Chair
Mr. RAHMANI Belkacem	M.C.B	Examiner
Mr. MOKRANI Lakhdar	Prof.	Supervisor
Mrs. BENLARBI Keltoum	M.C.B	Co-supervisor

Academic Year

2024/2025

ملخص:

تتناول هذه المذكرة مشكلة الاهتزازات الانزلاقية (*SSO*) المتكررة في أنظمة الحفر من خلال تطوير إطار تحكم ذكي يجمع بين النمذجة المتقدمة، التحكم الأمثل، والتلقين الآلي. تبدأ الدراسة بمراجعة نقدية لديناميكيات الحفر وطرق إخماد الاهتزازات الانزلاقية، مع تحديد أوجه القصور في الأساليب التقليدية. ثم تم تطوير نموذج التواء عالي الدقة بأربع درجات حرية (*4-DOF*) لمحاكاة دقيقة لسلوك هذه الاهتزازات، تلاه تصميم متحكم *LQR* معزز بعمل تكاملي للقضاء على أخطاء الحالة الدائمة أو المستقرة. ولتلبية متطلبات التطبيق العملي، تم دمج ملاحظ *Luenberger*لتقدير الحالات في الزمن الحقيقي.

بعد ذلك تم تحسين استراتيجية التحكم باستخدام تقنيات الذكاء الاصطناعي، حيث تقوم الخوارزميات الجينية (*GA*)بحساب مصفوفات الأوزان للمتحكم *LQR* لتحسين الأداء تحت ظروف اشتغال مختلفة، كما تم أيضا تدريب شبكة عصبونية اصطناعية (*ANN*) على ضبط معاملات التحكم ديناميكياً طبقا لظروف الحفر العشوائية في قعر البئر و ظروف اشتغال جهاز الحفر. أظهرت نتائج المحاكاة تحسناً كبيراً في إخماد الاهتزازات الانزلاقية، حيث تفوق متحكم *ANN-LQR* على المتحكمات التقليدية والمحسنة بالخوارزميات الجينية، خاصة في ظل الاضطرابات غير المتوقعة في ظروف الحفر.

توفر هذه الدراسة حلاً قوياً وقابلاً للتكيف للتخفيف من الاهتزازات الالتوائية في عمليات الحفر و جسراً بين التصميم النظري للتحكم والتطبيق العملي.

كلمات مفتاحية : ديناميكيات الحفر، نمذجة 4 درجات حرية، الاهتزازات الالتوائية، الاهتزازات الانزلاقية - (*SSO*) ، تحكم *LQR* - تحسين بالخوارزميات الجينية - (*GA*) ، الشبكات العصبونية الاصطناعية - (*ANN*) ، التحكم التكيفي، ظروف الحفر العشوائية في قعر البئر، التخفيف من الاهتزازات.

Abstract :

This dissertation tackles the persistent challenge of Stick-Slip Oscillations (*SSO*) in drilling systems by developing an intelligent control framework that combines advanced modeling, optimal control, and machine learning. The study begins with a review of drilling dynamics and *SSO* suppression methods, identifying limitations in conventional approaches. A high-fidelity 4-Degree-Of-Freedom (4-*DOF*) torsional model is then developed to accurately capture *SSO* behavior, followed by the design of a Linear Quadratic Regulator (*LQR*) enhanced with integral action to eliminate steady-state errors. To address practical implementation challenges, a *Luenberger* observer is integrated for real-time state estimation. The control strategy is further refined using computational intelligence techniques. Genetic Algorithms (*GA*) optimize the *LQR* weighting matrices to improve performance across diverse operating conditions, while an Artificial Neural Network (*ANN*) is trained to dynamically adjust control parameters in response to down-hole uncertainties. Simulation results demonstrate significant improvements in *SSO* suppression, with the *ANN*-adaptive *LQR* outperforming both conventional and *GA*-optimized *LQR* controllers, particularly under unpredictable disturbances and different operating conditions of the drilling system. This work provides a robust, adaptive solution for mitigating torsional vibrations in drilling operations, bridging the gap between theoretical control design and real-world applicability.

Key words: *Drilling dynamics, 4-DOF modeling, Torsional vibrations, Stick-slip oscillations* (*SSO*), *LQR control, Genetic Algorithm* (*GA*) *optimization, Artificial Neural Network* (*ANN*), *Adaptive control, Down-hole uncertainties, Vibration mitigation.*

Résumé :

Ce mémoire s'attaque au problème persistant des oscillations ‘stick-slip : *SSO*’ dans les systèmes de forage en développant une architecture de commande intelligente alliant modélisation avancée, commande optimale et intelligence artificielle. L'étude commence par une analyse critique des dynamiques de forage et des méthodes conventionnelles de suppression des *SSO*, mettant en lumière leurs limites. Un modèle torsionnel haute fidélité à 4 Degrés De Liberté (4-*DDL*) est ensuite développé pour caractériser précisément le phénomène *SSO*, suivi de la conception d'un régulateur *LQR* (*Linear Quadratic Regulator*) muni d’une action intégrale pour éliminer les erreurs en régime permanent. Un observateur de *Luenberger* est intégré pour l'estimation en temps réel des états, répondant ainsi aux contraintes pratiques d'implémentation. La stratégie de commande est ensuite optimisée via des techniques de l'intelligence artificielle. Les algorithmes génétiques (*AG*) ont été utilisés pour optimiser les matrices de pondération du régulateur *LQR* afin d’améliorer les performances dans diverses conditions de fonctionnement, tandis qu'un Réseau de Neurones Artificiels (*RNA*) adapte dynamiquement les paramètres de la commande aux incertitudes du fond de forage et aux conditions de fonctionnement du système. Les simulations démontrent une suppression significative des *SSO*, avec le régulateur adaptatif *RNA-LQR* surpassant les versions conventionnelle et optimisée par *AG*, notamment face aux perturbations imprévisibles. Ainsi, ce travail propose une solution robuste et adaptative pour atténuer les vibrations torsionnelles, combinant rigueur théorique et applicabilité industrielle.

***Mots clés**: Dynamique de forage, Modélisation de 4-DDL, Vibrations torsionnelles, Oscillations ‘stick-slip’* (*SSO*), *Commande LQR, Optimisation par algorithme génétique* (*GA*), *Réseau de Neurones Artificiels* (*RNA*), *Commande adaptative, Incertitudes du fond de forage, Réduction des vibrations.*

Dedication

*We dedicate this work to our **beloved families** the unwavering pillars of strength throughout our academic journey. Your unconditional love, constant encouragement, and steadfast belief in our potential have been the foundation on which we built every success.*

*We express our deepest appreciation to our **respected supervisor, Prof. MOKRANI Lakhdar**, whose exceptional guidance, expertise, and tireless support have significantly influenced our understanding of this field.*

*This memoir is also dedicated to all **individuals committed to advancing a more sustainable and innovative future** in the realm of automation and systems. May the insights and findings herein inspire and empower future colleagues to continue pushing the boundaries of theme.*

To every person who walked with us through this challenging path offering support, encouragement, and motivation we are deeply thankful. Your presence has been invaluable, and your belief in us, unforgettable.

Hakim & Mohamed Amine

Acknowledgment

First and foremost, we express our deepest gratitude to God for granting us faith, perseverance, and strength to complete this work.

We extend our sincere appreciation to ***Prof. MOKRANI Lakhdar****, our supervisor, for his invaluable guidance, patience, and dedication throughout the preparation of this dissertation. His insightful feedback and unwavering support were instrumental in shaping this work, and for that, we are profoundly grateful.*

Our thanks also go to ***Dr. Keltoum Benlarbi****, our co-supervisor, for her commitment and expertise. Her meticulous guidance, particularly in the modeling aspects of this research and writing review, was indispensable to its success.*

We are deeply honored by the time and effort invested by the members of the examination committee. Our sincere thanks go to ***Prof. BENMOUIZA Khalil****, President of the Jury, and* ***Dr. RAHMANI Belkacem****, Jury Member, for their thoughtful evaluation and constructive feedback on our work.*

We are also truly grateful to our families and friends for their constant support, motivation, and understanding throughout this period. Their presence made this achievement possible.

Finally, we would like to acknowledge all the teachers and all the staff of the ***Faculty of Technology*** *and the* ***Electrical Engineering Department*** *at* ***Laghouat University*** *for their continuous support and encouragement throughout our academic journey. Their contributions have greatly enriched our learning experience.*

Symbols & Acronyms List

Symbols & Acronyms List

- ***Symbols***

Symbol	***Signification***
A, B, C	State-space system matrices (state, input, output) respectively
$\bar{A}, \bar{B}$	Augmented state-space system matrices respectively
A_c, B_c, C_c	State-space matrices of the internal model respectively
c	Damping coefficient (general)
C_1, C_2	Damping matrices (local and mutual) respectively
$d(t)$	Disturbance vector
E, G	*Young*'s and *Shear* modulus respectively
$e(t)$	Tracking error
F	Force
H	Heaviside step function
J	Moment of inertia
J_r, J_p, J_c, J_b	Inertia of the rotary table, drill pipe, drill collar, and drill bit respectively
K	Stiffness matrix
K_x	Feedback gain matrix in *LQR* control
K_S, K_R	State feedback gain and internal model gain respectively
k	Stiffness factor/coefficient (general)
k_p, k_c, k_b	Torsional stiffness coefficients of pipe, collar, and bit sections respectively
L	Observer gain matrix; Length of the flexible section
M	Mass matrix
m	Mass
Q	State weighting matrix of the *LQR* control
R	Control input weighting matrix of the *LQR* control
R_b	Radius of the drill bit
$r(t)$	Reference signal

s	*Laplace* variable
T	Torque
$u(t)$	Control input vector; Axial displacement
$v(t), w(t)$	Lateral displacements respectively
$x(t)$	State vector
$\bar{x}(t)$	Augmented state vector
$\hat{x}(t)$	Estimated state vector
$\dot{x}, \ddot{x}$	First and second time derivatives respectively
$x_c(t)$	Internal model state
$y(t)$	System output vector
$\hat{y}(t)$	Estimated output vector
$z(t)$	Axial displacement of the bit
β	Zero-velocity threshold
γ_b	Parameter in the friction model
μ_{cb}, μ_{sb}	Friction coefficients
ξ	Random noise or fluctuation term
ρ	Mass density
φ, ϕ, θ	Angular displacements/positions
ω	Angular velocity

- ***Acronyms***

Acronym	***Signification***
AI	Artificial Intelligence
ANN	Artificial Neural Network
BHA	Bottom Hole Assembly
BOP	BlowOut Preventer
CBR	Case-Based Reasoning
DOF	Degree(s) Of Freedom
FEM	Finite Element Method
GA	Genetic Algorithm
IBOP	Internal BlowOut Preventer
ISE	Integral of Squared Error
LQR	Linear Quadratic Regulator
LWD	Logging While Drilling
MIMO	Multi-Input Multi-Output
MSE	Mean Squared Error
MWD	Measurement While Drilling
PGM	Power Generation Module
ReLU	Rectified Linear Unit
ROP	Rate Of Penetration
RPM	Revolutions Per Minute (used for rotary speed)
RSS	Rotary Steerable Systems
SVM	Support Vector Machine
ToB	Torque on Bit
USA	United States of America
WoB	Weight on Bit
PID	Proportional-Integral-Derivative

IoT	Internet of Things
FOPID	Fractional Order Proportional-Integral-Derivative
SSO	Self-Sustained Oscillations
LQG	Linear Quadratic Gaussian
SMC	Sliding Mode Control

Figures List

Figures List

Figure	Page
Chapter I Drilling Systems: A Review	
Figure I.1 Example of a manual percussion drilling	**7**
Figure I.2 A spring pole drilling mechanism	**7**
Figure I.3 A cable tool drilling	**8**
Figure I.4 An earlier rotary drilling tool	**9**
Figure I.5 A rotary table drilling with mud circulation	**9**
Figure I.6 A top drive system	**10**
Figure I.7 A drilling system allowing (MWD) & (LWD)	**11**
Figure I.8 A rotary steerable drilling system	**11**
Figure I.9 Offshore drilling rigs	**12**
Figure I.10 An *AI*-driven & automated drilling system	**13**
Chapter II Drilling Systems: Modeling & Control	
Figure II.1 a) An oil well drilling rig, b) A multi-*DOF* trosional model of the drill-string	**23**
Figure II.2 A 4-*DOF* torsional model of the drill-string	**26**
Figure II.3 Structure of the drill string control system	**29**
Chapter III Case Study of an LQR-based Control of a 4-DoF Drilling System	
Figure III.1 Structure of the investigated drill string control system	**39**
Figure III.2 Rotary table and bit speed vibration in stick-slip mode of operation of the drill string system	**41**
Figure III.3 Different operating modes of the drill-string system in the plan of (control torque T_m & WoB)	**42**
Figure III.4 Dynamic response of controlled drill string system (Reference, rotary table and bit speeds)	**43**

Figure III.5 *Luenberger* observer estimation of the drill string bit speed	**44**
Chapter IV Adaptive LQR Control via GA Optimization and ANN for Stick-Slip Mitigation	
Figure IV.1 Chromosome representation of the *Q* & *R* elements scaling factors	**48**
Figure IV.2 Flowchart of the working steps of *GAs*	**49**
Figure IV.3 Swapping genetic information after a single-point crossover process	**50**
Figure IV.4 Swapping genetic information after a two-point crossover process	**50**
Figure IV.5 Example of a displacement mutation	**51**
Figure IV.6 A simple inversion mutation	**51**
Figure IV.7 A scramble mutation	**52**
Figure IV.8 A multilayer perceptron	**52**
Figure IV.9 *ANN* training process	**53**
Figure IV.10 Dynamic response of the drill string system controlled by a basic *LQR*	**54**
Figure IV.11 *MATLAB* graphical interface '*gatool*' configuration & main settings	**56**
Figure IV.12 Dynamic response of the drill string system controlled by *GA-based LQR*	**57**
Figure IV.13 Dynamic response of the drill string system controlled by different *LQR-based techniques*	**58**
Figure IV.14 *MATLAB* graphical interface '*nntool*' configuration & main settings	**60**
Figure IV.16 Some *ANN* outputs and their targets	**61**

Tables List

Tables List

Table	Page
Chapter III Case Study of an LQR-based Control of a 4-DoF Drilling System	
Table III.1 Parameters of the 4-*DOF* torsional drill string model	**38**
Chapter IV Adaptive LQR Control via GA Optimization and ANN for Stick-Slip Mitigation	
Table IV.1 Cost function for different weighting factors cases	**56**
Table IV.2 *Different LQR* controller's robustness against operating conditions variation	**59**
Table IV.3 *Different LQR* controller's cost function comparison for some testing set points	**62**

Content

Title	Page
General Introduction	*1*
Chapter I Drilling Systems: A Review	5
I.1 INTRODUCTION	6
I.2 DRILLING SYSTEMS HISTORY	6
I.2.1. PERCUSSION DRILLING	6
I.2.1.1 MANUAL PERCUSSION DRILLING	6
I.2.1.2 SPRING POLE DRILLING	7
I.2.1.3 CABLE TOOL DRILLING	7
I.2.2. ROTARY DRILLING	8
I.2.2.1 EARLY ROTARY DRILLING	8
I.2.2.2 ROTARY TABLE DRILLING WITH MUD CIRCULATION	9
I.2.2.3 TOP DRIVE SYSTEM	10
I.2.3. DIRECTIONAL DRILLING	10
I.2.3.1 MEASUREMENT AND LOGGING WHILE DRILLING	10
I.2.3.2 ROTARY STEERABLE SYSTEMS	11
I.2.4. OFFSHORE DRILLING RIGS	12
I.2.5. AI-DRIVEN AND AUTOMATED DRILLING SYSTEMS	12
I.3. DRILL-STRING MODELING	13

I.3.1. FINITE ELEMENT METHOD	13
I.3.2. LUMPED PARAMETERS MODELS	14
I.3.3. COSSERAT THEORY	14
I.3.4. ANALYTICAL – NUMERICAL MODELS	14
I.3.5. NONLINEAR STOCHASTIC DYNAMICS	15
I.3.6. 4N-DOF DRILL STRING MODEL	15
A) AXIAL DYNAMICS	15
B) TORSIONAL DYNAMICS	16
C) LATERAL DYNAMICS	16
D) ANGULAR BENDING	16
E) NON-LINEARITIES	16
I.4. DRILL STRING CONTROL	17
I.4.1. TRADITIONAL TECHNIQUES	17
I.4.2. INTELLIGENT TECHNIQUES	17
I.4.2.1. ARTIFICIAL INTELLIGENT TECHNIQUES	18
I.4.2.1.1. ARTIFICIAL NEURAL NETWORKS	18
I.4.2.1.2. FUZZY LOGIC	18
I.4.2.1.3. OPTIMIZATION ALGORITHMS	18
I.4.2.1.4. SUPPORT VECTOR MACHINES	19
I.4.2.1.5. CASE-BASED REASONING	19
I.4.2.1.6. HYBRID TECHNIQUES	19
I.4.3. AUTOMATED TOP DRIVE SYSTEMS	19

I.4.4. ADAPTIVE ANTI-STICK-SLIP AND VIBRATION DAMPERS	20
I.5 CONTROL TECHNIQUES FOR STICK-SLIP OSCILLATION SUPPRESSION	20
I.6.CONCLUSION	21
Chapter II Drilling Systems: Modeling & Control	22
II.1 INTRODUCTION	23
II.2. DRILL STRING MODELING	23
II.2.1. MULTI-*DoF* TORSIONAL MODEL OF A DRILL STRING	24
II.2.2. 4-*DoF* TORSIONAL MODEL OF A DRILL STRING	27
II.2.3. MODELING OF THE TORQUE BIT BEHAVIOR	29
II.3. DRILL STRING CONTROL STRATEGY FOR STICK-SLIP VIBRATION MITIGATION	30
II.3.1. STATE SPACE OBSERVER	31
II.3.2. *LQR* OPTIMAL CONTROL	32
II.3.3. INTERNAL MODEL	33
II.3.4. WEIGHTING MATRICES TUNING AND CONTROL EFFECTIVENESS	*34*
II.4. CONCLUSION	34
Chapter III Case Study of an LQR-based Control of a 4-DoF Drilling System	36
III.1.INTRODUCTION	36
III.2. CASE STUDY SYSTEM DESCRIPTION	36
III.2.1. DRILLING SYSTEM CONFIGURATION	36
III.2.2. PARAMETERS OF THE 4-*DoF* TORSIONAL MODEL	36

III.3. *LQR* CONTROL & OBSERVER IMPLEMENTATION AND PARAMETERS TUNING	**37**
III.3.1 *LQR* PARAMETERS TUNING	**39**
III.3.2 OBSERVER PARAMETERS TUNING	**39**
III.4. SIMULATION RESULTS AND ANALYSIS	**39**
III.4.1. OPEN-LOOP SYSTEM BEHAVIOR	**40**
III.4.2. CLOSED-LOOP SYSTEM BEHAVIOR AND PERFORMANCE	**42**
III.4.3. OBSERVER PERFORMANCE	**42**
III.5. CONCLUSION	**43**
Chapter IV Adaptive LQR Control via GA Optimization and ANN for Stick-Slip Mitigation	**45**
IV.1.INTRODUCTION	**46**
IV.2 METHODOLOGY	**46**
IV.2.1. CONVENTIONAL *LQR* CONTROL REVIEW	**47**
IV.2.2. *GA*-BASED OPTIMIZATION OF *LQR*	**47**
IV.2.2.1 GENETIC ALGORITHM PRINCIPLE	**47**
IV.2.2.2 CHROMOSOMES REPRESENTATION	**48**
IV.2.2.3 WORKING STEPS OF THE GENETIC ALGORITHM	**48**
IV.2.3 *ANN*-BASED ADAPTIVE *LQR*	**52**
IV.2.3.1 *ANN* architecture	**52**
IV.2.3.2 Training algorithm	**53**
IV.2.3.3 Real-time adaptation	**54**

IV.3 SIMULATION RESULTS AND ANALYSIS	**54**
IV.3.1 CONVENTIONAL *LQR*	**54**
IV.3.2 *GA*-Optimized *LQR*	**55**
IV.3.3 *ANN*-based adaptive *LQR*	**59**
IV.3.4 COMPARATIVE PERFORMANCE OF DIFFERENT *LQR*-BASED CONTROLLERS	**61**
IV.4. CONCLUSION	**62**
General Conclusion	**63**
Bibliography	**66**

General Introduction

General Introduction

Drilling systems are critical in the oil and gas industry, enabling hydrocarbon extraction from subsurface reservoirs. However, drilling operations often face challenges such as stick-slip oscillations (*SSO*) – a severe torsional vibration phenomenon that reduces drilling efficiency, damages equipment, and increases operational costs [1],[2]. *SSO* occur when the drill bit intermittently sticks and slips due to friction, leading to irregular rotational speeds and excessive torque fluctuations [3].

To mitigate *SSO*, advanced modeling and control techniques are employed. Traditional approaches include passive damping solutions, while modern methods leverage active control strategies such as Linear Quadratic Regulator (*LQR*), adaptive control, and intelligent optimization algorithms [6],[7]. The integration of machine learning and evolutionary algorithms further enhances control robustness under varying drilling conditions.

The motivation behind this research arises from:

- The need for efficient *SSO* mitigation to improve drilling performance and equipment longevity [8].
- The limitations of conventional control methods in handling nonlinearities and uncertainties in drilling dynamics [9].
- The potential of artificial intelligence (*AI*)-based optimization to enhance controller adaptability under different operating conditions [10].
- The industrial demand for cost-effective and reliable automated drilling solutions [11].

Consequently, here are the main objectives of this dissertation:

- Develop a high-fidelity four-Degree Of Freedom (4-*DOF*) drilling model capturing torsional dynamics and stick-slip behavior.
- Design an *LQR* controller with integral action to regulate rotary table speed and suppress *SSO*.
- Optimize *LQR* weighting matrices (*Q* & *R*) using Genetic Algorithms (*GA*) to minimize the Integral Squared Error (*ISE*) of rotary and bit speeds.

- Implement an Artificial Neural Network (*ANN*)-based adaptive *LQR* to dynamically adjust control parameters for varying operating conditions.
- Compare the performance of conventional *LQR*, *GA*-optimized *LQR*, and *ANN*-based *LQR* through simulations.

The dissertation is organized into four cohesive chapters, each building upon the previous to present a comprehensive study on drilling system modeling and stick-slip oscillation mitigation.

The first chapter establishes the foundational context by reviewing the evolution of drilling systems, from early mechanical approaches to modern automated techniques. It systematically examines prevalent modeling methodologies, including lumped-parameter and finite element models, while critically analyzing conventional and advanced control strategies employed for *SSO* suppression. This literature review not only identifies gaps in existing solutions but also justifies the need for intelligent control integration in drilling operations.

The second chapter transitions from theory to implementation by developing a detailed 4-*DoF* torsional drilling model that captures the essential dynamics of stick-slip phenomena. Here, the design and implementation of an *LQR* controller augmented with integral action are presented, addressing steady-state error limitations of standard *LQR*. To enable practical deployment, a *Luenberger* observer is incorporated for real-time state estimation, ensuring robustness against measurement constraints. This chapter bridges modeling and control, setting the stage for subsequent optimization.

The third chapter shifts focus to empirical validation through a structured case study. The drilling system parameters are defined, and the control architecture of Chapter 2 is applied. A comparative analysis of open-loop and closed-loop simulations highlights the uncontrolled system's vulnerabilities and the *LQR* controller's efficacy in stabilizing torsional vibrations. These results serve as a baseline for the advanced optimization and intelligent adaptive methods introduced later.

The final chapter elevates the control strategy through computational intelligence. Genetic Algorithms are employed to optimize the *LQR*'s Q and R matrices, minimizing performance indices across diverse operating conditions.

Building on this, an Artificial Neural Network is designed and trained to dynamically adapt control parameters, ensuring robustness against down-hole uncertainties and operating conditions variation. The chapter culminates in a performance comparison of the three control paradigms (Conventional *LQR*, *GA*-optimized *LQR*, and *ANN*-adaptive *LQR*) demonstrating the progressive enhancement in *SSO* suppression.

Together, these chapters form a global framework that advances drilling automation through synergistic integration of control theory, evolutionary computation, and machine learning. Thus, this study contributes to improve drilling efficiency and reliability by combining these modern techniques, paving the way for smarter and more adaptive drilling automation systems.

Chapter I

Drilling Systems:

A Review

I.1 INTRODUCTION

Drilling systems have undergone significant advancements in recent decades, driven by technological innovations, automation and the need for enhanced efficiency, safety and sustainability.

In this chapter, we will present a review on drilling systems history, drill-string modeling and control. This review explores mainly the latest developments in drilling technologies and focuses on modern drilling techniques, automation, real-time monitoring and sustainability considerations.

I.2 DRILLING SYSTEMS HISTORY

Drilling systems can be classed and ranked in a chronological way, tracing their evolution from primitive manual methods to advanced automated technologies. Early drilling, dating back thousands of years, involved simple tools like hand-operated augers and percussion mechanisms used for water wells and mining. The 19th century saw the rise of mechanical rotary drilling, revolutionizing oil and gas extraction with the advent of the first steam-powered rigs. The 20th century introduced hydraulic systems, diamond drill bits, and offshore drilling platforms, while modern advancements now incorporate computerized automation, directional drilling, and eco-friendly technologies, marking a continuous progression in efficiency and precision. In this section, these different generations of drilling systems will be presented briefly.

I.2.1 PERCUSSION DRILLING

Percussion drilling is one of the oldest and most straightforward drilling methods, relying on repeated impacts to break and penetrate rock formations. It evolved from simple manual techniques to advanced mechanized systems. Ancient civilizations used rope-and-pulley percussion to dig water wells, repeatedly lifting and dropping a heavy tool to break rock. By the 19th century, cable-tool drilling (or ‘spudder’ rigs) became the standard, using steam or internal combustion engines to automate the pounding action for oil and water wells. The early 20th century introduced pneumatic percussion drills, powered by compressed air, revolutionizing mining and construction. Later, Down-The-Hole (*DTH*) hammers emerged, integrating the hammer directly into the drill string for deeper, more efficient drilling. Today, percussion systems incorporate hydraulic power, advanced materials, and automation, remaining vital in mineral exploration, geothermal drilling, and well construction.

I.2.1.1 MANUAL PERCUSSION DRILLING

It is one of the earliest drilling methods (In ancient times – 19th century), used by civilizations such as the Chinese (2000 *BCE*), Egyptians, and Romans. A heavy tool was manually lifted and dropped to break the rock through repetitive strikes (see figure I.1).

Chinese ‘Deep Well Drilling’ (~2000 *BCE*) used bamboo pipes to extract water, with wells reaching 500 meters deep.

Roman Water Wells (~500 *BCE* – 500 *CE*) used basic percussion techniques to dig wells for water supply.

European Mining Wells (Middle Ages) utilized hand-powered wooden drill rigs for salt and mineral extraction [12].

This kind of drilling system is an extremely slow process that could not drill deep enough for commercial oil and gas extraction.

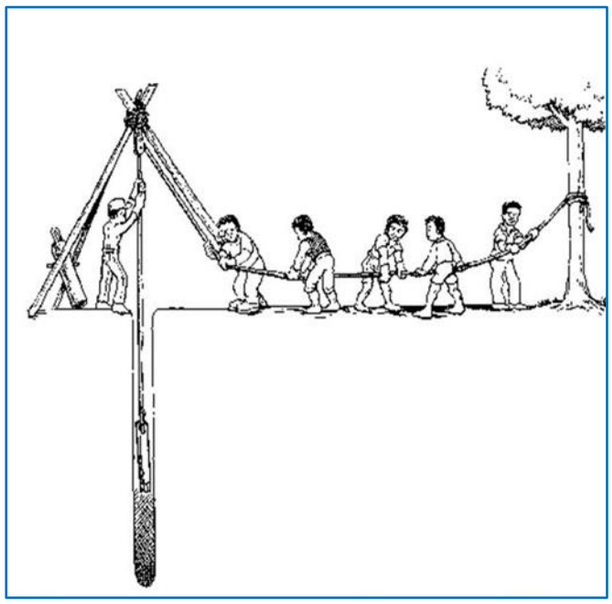

Figure I.1 Example of a manual percussion drilling [13]

I.2.1.2 Spring Pole Drilling

It was an improved form of percussion drilling (that has been appeared in early 1800s) where a bent wooden pole provided additional mechanical leverage (see figure I.2). It is used in early water well drilling and salt mining [14]. It allowed for deeper wells compared to manual percussion. But it required a lot of manual labor. Its limited depth capability is about (~30–50 meters).

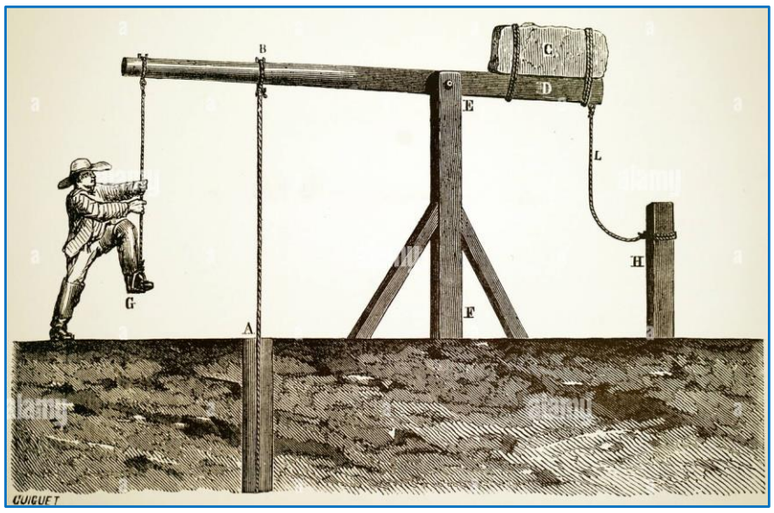

Figure I.2 A spring pole drilling mechanism [15]

I.2.1.3 Cable Tool Drilling

Also known as ‘spudding’, this method (Mid – 1800s) involved lifting and dropping a chisel-shaped drill bit with a cable to fracture the rock. It is first used commercially in oil well drilling.

The *Edwin Drake's* is the first commercial oil well (1859, Pennsylvania-USA), it used a cable tool drilling that could drill up to 600 meters deep and it allowed well casing installation, preventing collapse [16].

In counterpart, it was extremely slow and could take months to drill a single well. Moreover, it required bailing out cuttings manually.

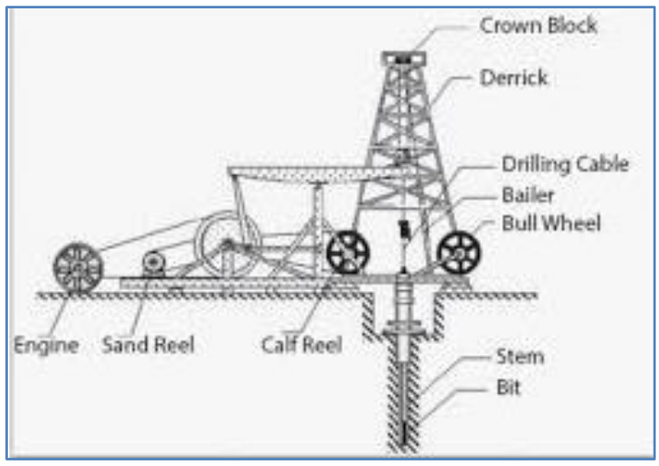

Figure I.3 A cable tool drilling [17]

I.2.2 ROTARY DRILLING

The history of rotary drilling systems traces back to ancient times when manual rotary tools were used for simple boreholes, but the modern era began in the 19th century with the development of mechanical rotary rigs for oil exploration. Early rotary systems used a rotating bit to cut through rock, replacing the slower percussion methods. The introduction of roller-cone bits in the early 1900s significantly improved efficiency, while later advancements included diamond-impregnated bits for hard formations. Offshore drilling emerged in the mid-20th century with floating rigs and directional drilling technology, allowing wells to be drilled at different angles. Today, rotary systems incorporate automated top drives, Polycrystalline Diamond Compact (*PDC*) bits, and real-time data monitoring, making them faster, more precise, and adaptable to extreme environments.

I.2.2.1 EARLY ROTARY DRILLING

Unlike percussion drilling, rotary drilling (appeared in late 1800s to early 1900s) used a rotating bit to cut through rock continuously. Initially, it is powered by steam engines and later replaced by internal combustion engines. It is first used in *Texas - USA* (1901, *Spindletop Oil Gusher*) [18].

It allowed continuous drilling without stopping and it could drill deeper and faster than cable tool drilling. Besides, it used multiple drill bits (roller cone bits, drag bits) for different formations, see figure I.4.

On the other hand, it required manual handling of drill pipes and it lacked control over drilling direction.

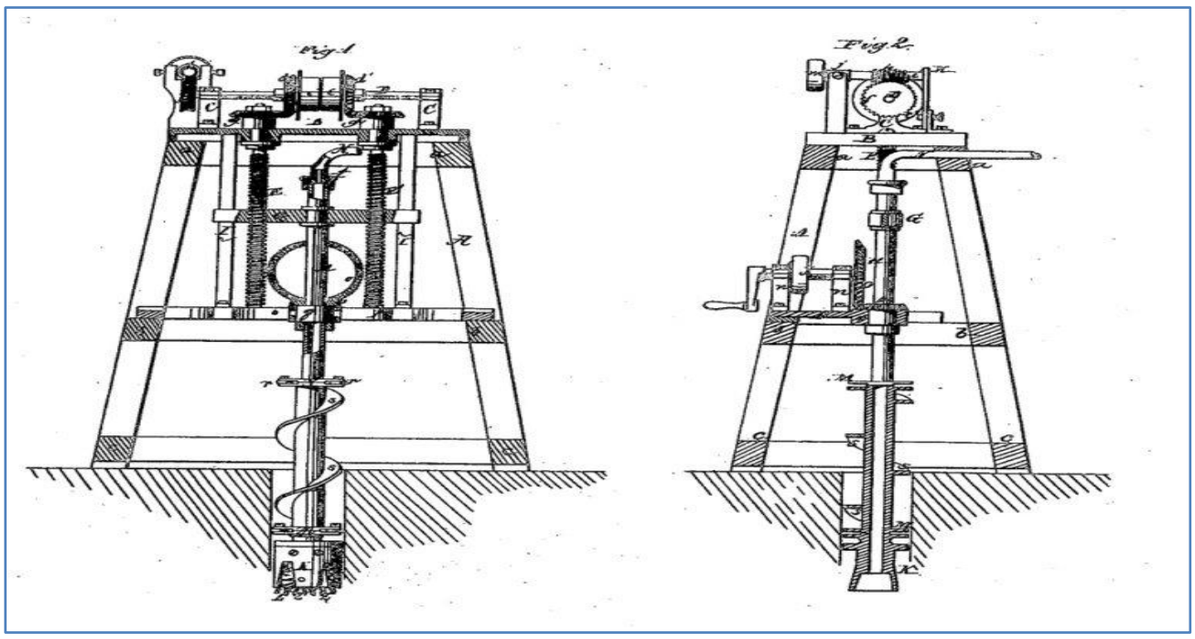

Figure I.4 An earlier rotary drilling tool [19]

I.2.2.2 Rotary Table Drilling with Mud Circulation

It introduced the rotary table (Early 1900s) and it allowed the drill string to be rotated more efficiently. Besides, it used drilling mud (fluid) to cool the bit, lubricate the drill pipe and carry cuttings to the surface, see figure I.5.

This drilling mud system improved well stability and bit cooling and the rotary table system allowed deeper and faster drilling. Consequently, it improved well control and reduced wellbore collapses. Elsewhere, a Blow Out Preventer (*BOP*) was developed in the 1920s to improve safety.

In counterpart, it still required manual pipe handling and couldn't provide real-time down-hole data [20].

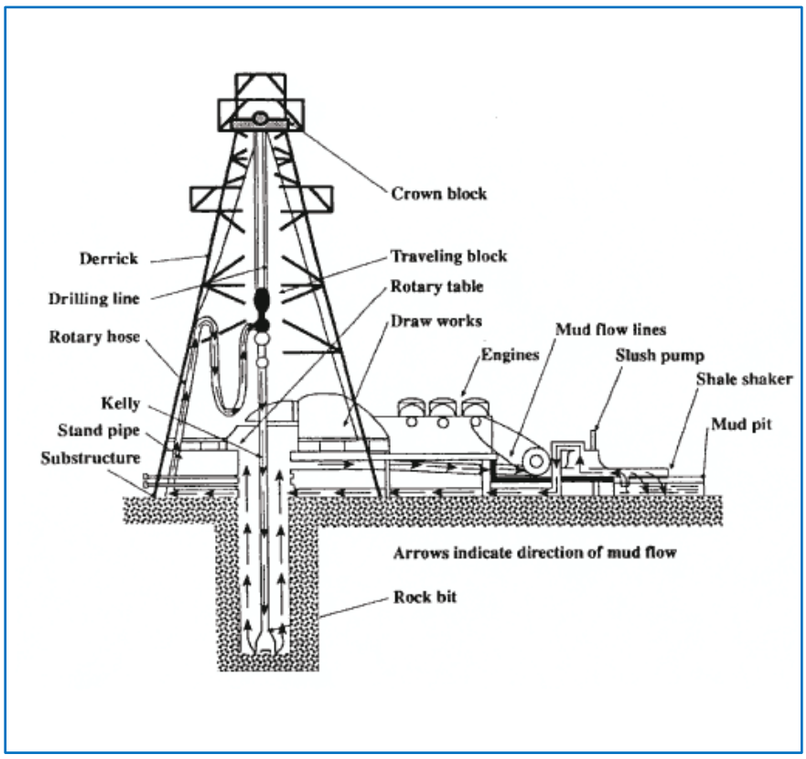

Figure I.5 A rotary table drilling with mud circulation [21]

I.2.2.3 TOP DRIVE SYSTEM

It was developed in 1970s to replace rotary tables, allowing drill pipes to be connected without stopping the rotation [22]. It allowed faster and safer drilling without need to stop for pipe connections. Moreover, it reduced risk of stuck pipes and improved automation in drilling operations. But, it was expensive to implement on older rigs.

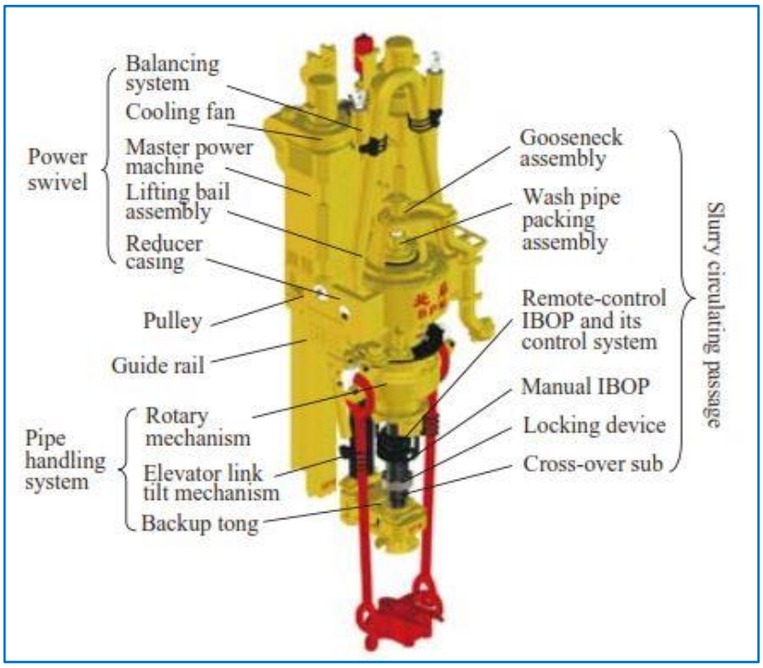

Figure I.6 A top drive system [23]

I.2.3 DIRECTIONAL DRILLING

Directional drilling traces its origins to the 1920s when innovators first experimented with controlled wellbore deviations to access multiple reservoirs from a single location. Early techniques relied on deflection wedges (whipstocks) and bent housings, but progress accelerated in the 1930s with the introduction of down-hole mud motors and Measurement-While-Drilling (*MWD*) tools. The 1970s and 1980s saw breakthroughs in Rotary Steerable Systems (*RSS*) and 3D seismic imaging, enabling precise well paths in complex formations. Today, directional drilling is essential in offshore, shale, and extended-reach projects, integrating real-time data analytics, automated steering, and ultra-precise geosteering to maximize efficiency and minimize environmental impact.

The key advancements of this kind of drilling, that enables drilling at non-vertical angles to reach complex reservoirs, are summarized hereafter.

I.2.3.1 MEASUREMENT AND LOGGING WHILE DRILLING

Appeared in (1980s – 1990s), these advanced tools (Measurement While Drilling (*MWD*) & Logging While Drilling (*LWD*)) have been used to collect down-hole data in real-time, enabling better well planning and decision-making [24], [25].

The main key Innovations of these drilling systems are:

- Real-time well trajectory control
- Improved safety and drilling accuracy
- And better decision-making during drilling.

But, it presents some limitations such as:

- It is expensive to implement
- It requires trained personnel to interpret data.

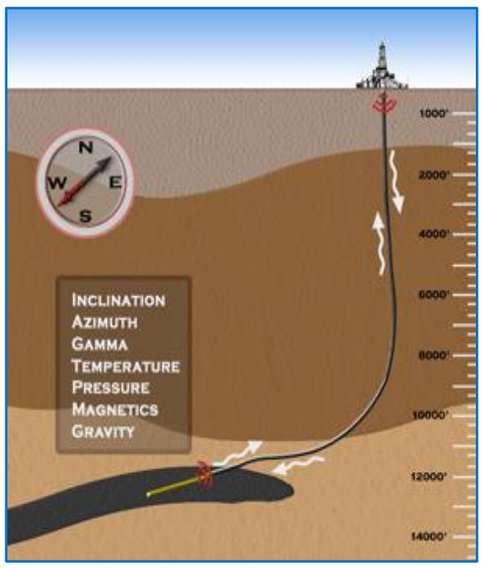

Figure I.7 A drilling system allowing (MWD) & (LWD) [26]

I.2.3.2 ROTARY STEERABLE SYSTEMS

The Rotary Steerable System (*RSS*) is an advanced directional drilling system that allows precise wellbore placement without stopping rotation, improving directional drilling accuracy [27]. It appeared in (1990s – 2000s) and it is characterized by the following key innovations:

- It allowed drilling of horizontal and complex wells
- It has faster penetration rates and higher precision
- It is used in unconventional oil and gas drilling (shale gas, deepwater)
- In counterpart, it has high operational costs.

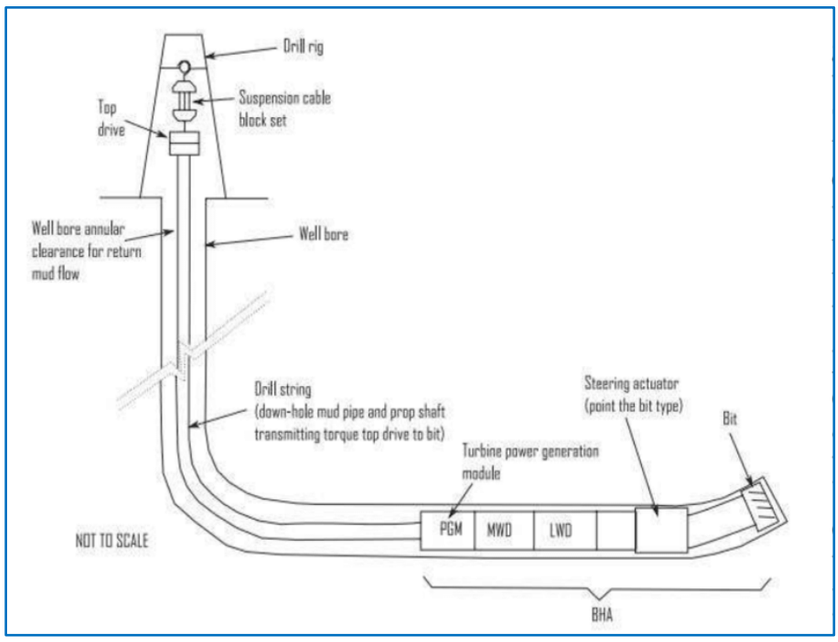

Figure I.8 A rotary steerable drilling system [28]

I.2.4 OFFSHORE DRILLING RIGS

In (1940s – 1950s), floating and fixed offshore drilling platforms to explore oil in deepwater have been developed [29]. Here are some key innovations of this kind of modern infrastructures:

- First fixed offshore platform (1947, *Gulf of Mexico - USA*)
- Jack-up rigs that are movable platforms that could drill in shallow waters
- Semi-submersible rigs that are used in deeper water and provide stability.

These offshore drill systems have some limitations, we mainly state:

- Requirement of heavy investment and complex logistics
- Environmental risks such as oil spills.

Figure I.9 An offshore drilling rigs [30]

I.2.5 *AI*-DRIVEN AND AUTOMATED DRILLING SYSTEMS

From 2010s until now, automation and *AI*-driven analytics are transforming drilling operations by optimizing performance and reducing human intervention.

Here are some key innovations of this kind of sophisticated drilling systems:

- Autonomous drilling rigs that adjust drilling parameters in real-time
- *AI*-driven optimization allowing reducing drilling costs and risks
- Geothermal and ultra-deepwater drilling advancements.

In counterpart, these systems have the following main limitations:

- High initial investment
- Requirement of digital infrastructure.

Figure I.10 An *AI*-driven & automated drilling system [31]

I.3 DRILL-STRING MODELING

Drill-string modeling employs advanced mathematical techniques to predict and estimate dynamic behavior, including vibrations, stick-slip and bit-bounce. Below are summarized the key modeling approaches with their governing equations.

I.3.1 FINITE ELEMENT METHOD

The finite Element Method (*FEM*) discretize the drill-string geometry into elements, and the dynamic response is computed using partial differential equations of motion.

Here is the governing equation (*Timoshenko* beam model) [32]:

$$\rho A \frac{\partial^2 u}{\partial t^2} - \frac{\partial}{\partial x}\left(EA \frac{\partial u}{\partial x}\right) = f(x,t)$$
$$\rho J \frac{\partial^2 \theta}{\partial t^2} - \frac{\partial}{\partial x}\left(GI_p \frac{\partial \theta}{\partial x}\right) + kGA\left(\frac{\partial \omega}{\partial x} - \theta\right) = 0 \quad \text{(I.1)}$$

With:

u, ω: Axial and lateral displacements

θ: Rotation angle

E, G: *Young*'s and shears modulus

ρ: Mass density

k: Shear correction factor

A, J, I_p: Cross-sectional area, moment of inertia and polar moment respectively.

$f(x,t)$: distributed axial force per unit length (e.g., drilling forces, friction, fluid drag)

I.3.2 LUMPED PARAMETER MODELS

In this case, the drill-string is simplified into mass-spring-damper systems for real-time control purposes. Here is the torsional stick-slip basic model of a drilling string [33]:

$$J\frac{d^2\theta}{dt^2} + c\frac{d\theta}{dt} + k\theta = T_{drive} - T_{bit} \tag{I.2}$$

Where:

J is the moment of inertia

c is the damping coefficient

k is the stiffness factor

T_{bit} is a nonlinear bit-rock interaction torque

T_{drive} is the driving torque.

In order to take into account, the axial-lateral-torsional coupling, one can use the more general following model:

$$M\ddot{q} + C\dot{q} + Kq = F_{ext} \tag{I.3}$$

Where $q = [u\ \omega\ \theta]^T$ is the vector of displacements and F_{ext} is the vector of external forces and moments.

M: Global mass matrix

C: Global damping matrix

K: Global stiffness matrix

I.3.3 COSSERAT THEORY

In this case, the drill-string model is a continuous rod with bending, torsion and shear effects. Here are the balance equations [34]:

$$\begin{aligned} \rho A\frac{\partial^2 r}{\partial t^2} &= \frac{\partial n}{\partial s} + F_{ext} \\ \rho J\frac{\partial^2 \theta}{\partial t^2} &= \frac{\partial m}{\partial s} + \frac{\partial r}{\partial s} \times n + M_{ext} \end{aligned} \tag{I.4}$$

With:

n, m: Internal forces and moments

F_{ext}, M_{ext}: External distributed forces and moments

r, θ: Position and rotation position vectors

s: Arc-length coordinate along the rod

I.3.4 ANALYTICAL–NUMERICAL MODELS

This approach combines differential equations with numerical solvers of contact and friction problems. It allows to take into account the sever non-linearity of the model (especially the torque on the drilling string bit).

Hereafter, we give the model of the torque resulting from the bit-rock interaction [35]:

$$T_{bit} = ROP \times \mu \times WOB \quad \text{(I.5)}$$

Where:

ROP :is the Rate Of Penetration

μ : is the friction coefficient

$WoB:$ is the Weight On Bit

Moreover, here is the borehole contact model [35]:

$$F_{contact} = [K_c(r - r_{well}) + C_c(\dot{r} - \dot{r}_{well})] \times H(r - r_{well}) \quad \text{(I.6)}$$

With:

K_c : The contact stiffness coefficient

C_c: The contact damping coefficient

r: The position of the drill string

r_{well}: The position of the borehole wall

H: *Heaviside* step function ensuring that damping only acts during contact.

I.3.5 NONLINEAR STOCHASTIC DYNAMICS

This approach incorporates uncertainties like random rock strength to model the torque on the bit. For example, here is a stochastic stick-slip model [36]:

$$J\,\ddot{\theta} + c\,\dot{\theta} + k\theta = T_{bit}(\theta(t), \dot{\theta}(t), \xi(t)) \quad \text{(I.7)}$$

Where $\xi(t)$ represents noise or random fluctuations.

I.3.6 *4-DOF* DRILL STRING MODEL

A *4-DOF* drill string model refers to a dynamic model used in drilling engineering to simulate the behavior of a drill string with four Degrees of Freedom (*DOF*) per node, where *n* is the number of nodes or segments into which the drill string is discretized. [37] This kind of models is used to capture complex mechanical interactions in rotary drilling, especially for trajectory control and vibration analysis.

Here are the degrees of freedom in a *4-DOF* model:

1. Axial displacement $u(z,t)$ which is the longitudinal motion along the drill string
2. Lateral displacement $v(z,t)$ which is sideways bending of the drill string
3. Torsional displacement $\theta(z,t)$ that characterizes the rotation around the drill string axis
4. Angular deflection $\phi(z,t)$ in lateral plane due to bending.

And here are the motion equations in this case [37]:

a) Axial Dynamics:

$$m_z\ddot{z}(t) + c_z\,\dot{z}(t) + k_z\,z(t) = F_{wob} - F_B(z, \dot{z}) \quad \text{(I.8)}$$

With:

m_z: The axial mass

c_z: The axial damping coefficient

k_z: The axial stiffness

F_{wob}: The weight on the bit

F_B: The bit-rock interaction force (nonlinear)

$z(t)$: The axial displacement of the bit (positive downwards)

b) Torsional dynamics:

$$J\,\ddot{\theta}(t) + c_\theta\dot{\theta}(t) + k_\theta\theta(t) = T_D - T_B(\theta, \dot{\theta}) \quad \text{(I.9)}$$

Where:

J: is the moment of inertia

c_θ: is the torsional damping

k_θ: is the torsional stiffness

T_D: is the applied torque from top drive

T_B: is the bit-rock torque interaction (nonlinear friction torque)

c) Lateral dynamics

- **In *X*-direction :** $m\ddot{x}(t) + c_l\dot{x}(t) + k_l x(t) = F_{lx}(x, \dot{x})$ (I.10)
- **In *Y*-direction:** $m\ddot{y}(t) + c_l\dot{y}(t) + k_l y(t) = F_{ly}(y, \dot{y})$ (I.11)

Where:

$x(t), y(t)$ are the lateral displacements in orthogonal horizontal directions

m is the lateral mass at the bit

c_l is the lateral damping factor

k_l is the lateral stiffness (bending stiffness of string)

F_{lx}, F_{ly} are the nonlinear lateral contact/friction forces that depend on borehole shape, formation, contact model.

d) Angular bending:

$$\phi_x(t) = \frac{L_x(t)}{L}, \phi_y(t) = \frac{L_y(t)}{L} \quad \text{(I.12)}$$

With:

$\phi_x(t), \phi_y(t)$: the angular deflections (slopes) in *x-z* and *y-z* planes

$L_x(t), L_y(t)$: the lateral displacements at the bit

L: the length of the flexible section of the drill string.

e) Nonlinearities: The model often includes nonlinearities in:

- Bit–rock interaction forces/torques
- Friction (especially in torsional model)
- Clearance and contact forces (in lateral model)
- Coupling between degrees of freedom.

I.4 DRILL STRING CONTROL

Controlling a drilling string system is a critical aspect of modern oil and gas drilling operations, ensuring safety, efficiency and optimal performance during wellbore construction [38].

Traditional methods often struggle with dynamic down-hole conditions, leading to inefficiencies. *AI* techniques offer a promising solution by enabling adaptive, data-driven control strategies that can predict and respond to complex behaviors like stick-slip and vibrations in real time, improving performance and reducing non-productive time.

I.4.1 TRADITIONAL TECHNIQUES

Traditional drill string control techniques have formed the backbone of drilling operations for decades, relying on mechanical systems and operator expertise to manage drilling parameters. The primary methods include rotary table systems, top drive assemblies, stabilizers, and manual Weight-On-Bit (*WoB*) adjustments. Rotary tables, the earliest form of drill string rotation, provided basic rotational control but lacked precision, often leading to inconsistent torque management and increased wear. The introduction of top drive systems in the late 20th century marked a significant improvement, enabling continuous rotation and circulation while tripping, yet still required manual intervention for optimal performance.

Stabilizers and reamers were used to maintain wellbore trajectory and reduce vibrations, but their passive nature limited adaptability to changing down-hole conditions. Jarring devices, another traditional tool, helped free stuck pipe but relied on reactive measures rather than preventive control. These techniques were heavily dependent on driller experience, often resulting in inefficiencies such as excessive vibration, stick-slip, and suboptimal Rate of Penetration (*ROP*).

While these methods were effective for conventional vertical wells, their limitations became apparent in complex formations and directional drilling. The lack of real-time data and automated adjustments often led to wellbore instability, equipment fatigue, and non-productive time. Despite these drawbacks, traditional control techniques remain relevant in low-cost, straightforward drilling operations. However, the industry's shift toward automated systems (equipped with down-hole sensors, real-time monitoring, and closed-loop control) has rendered many traditional approaches obsolete for high-precision applications. They played an essential role in laying the groundwork for modern advancements in drill string technology.

I.4.2 INTELLIGENT TECHNIQUES

Intelligent controllers in modern drill string systems leverage advanced algorithms, real-time data analytics, and machine learning to optimize drilling operations, enhance safety, and reduce costs. These controllers autonomously adjust drilling parameters (such as weight on bit, torque, and rotational speed) based on down-hole conditions, improving efficiency and mitigating risks like stick-slip vibrations or wellbore instability. Integrated with Internet of Things (*IoT*) and cloud computing, they enable predictive maintenance and remote monitoring, ensuring adaptive decision-making in complex geological environments. By minimizing human intervention and maximizing precision, intelligent controllers represent a transformative shift toward smarter, more reliable drilling technologies.

Modern drill string systems leverage *AI*-driven automation, real-time data analytics, and adaptive control algorithms to optimize drilling performance. Key intelligent controllers include:

I.4.2.1 ARTIFICIAL INTELLIGENCE TECHNIQUES

Artificial Intelligence (*AI*) has become increasingly important in petroleum exploration and production since its first application in 1989. It has been applied to overcome challenges such as seismic pattern recognition, reservoir characterization, drill bit diagnosis, and production optimization.

Its key strengths include learning from examples, handling noisy data, solving nonlinear problems, and making fast, generalized predictions once trained.

Moreover, the *AI* techniques help reduce operational costs, enhance decision-making, and improve safety and efficiency. Here are the main used techniques in the drilling systems:

I.4.2.1.1 ARTIFICIAL NEURAL NETWORKS

The Artificial Neural Networks (*ANNs*) are used for drill bit selection, gradient prediction, casing collapse prediction, bit wear control, drag/load prediction, vibration control, kick monitoring, and stuck pipe prediction.

These intelligent techniques can handle nonlinear data, learn from large datasets and make fast predictions once trained.

For example, *ANNs* have been used to monitor bottom hole assembly and detect down-hole conditions in real time based on inputs like *WoB*, *RPM* and mud properties.

I.4.2.1.2 FUZZY LOGIC

Fuzzy logic is an effective intelligent technique used to handle uncertainty and imprecise information, common in down-hole environment. It allows for rule-based control using linguistic inputs, making it ideal for adaptive drilling control where precise mathematical models are unavailable. It is applied in well stability assessment, drilling optimization, and early risk detection.

Its main strengths are imprecise handling, vague input data treating using rule-based systems, it ability to mimic human decision-making.

It can be applied, for example, for formation evaluation and real-time control where precise models are not available (like drilling systems) [39].

I.4.2.1.3 OPTIMIZATION ALGORITHMS

Modern drill string systems increasingly rely on advanced optimization algorithms to enhance performance, efficiency, and reliability in challenging drilling environments. Techniques such as Genetic Algorithms (*GA*), Particle Swarm Optimization (*PSO*), gradient-based methods …, are used to fine-tune control parameters, minimizing vibrations, reducing energy consumption, and preventing drill bit damage. Model Predictive Control (*MPC*) and Reinforcement Learning (*RL*) leverage real-time data to dynamically optimize weight-on-bit, rotational speed, and directional drilling paths.

Additionally, machine learning-driven surrogate models accelerate decision-making by approximating complex down-hole dynamics, enabling faster adjustments. These algorithms improve drilling accuracy, extend equipment lifespan, and reduce operational costs, making them essential for intelligent and automated drilling systems.

By carrying optimal solution over large solution spaces, these algorithms are good for complex and/or nonlinear problems. They have been used to plan optimal well trajectories and for platform selection in deepwater drilling.

I.4.2.1.4 SUPPORT VECTOR MACHINES

Support vector machines (*SVMs*) are employed for classification and regression in drilling operations. They are used to detect drilling (normal and faulty) states, predict outcomes like bit wear or pressure gradients, and model relationships with high accuracy and low training time, even in noisy environments. *SVM*s are known for their high accuracy, fast training, good generalization on small or noisy datasets. They help classify drilling states and predict faults more reliably than traditional methods [39].

I.4.2.1.5 CASE-BASED REASONING

Case-Based Reasoning (*CBR*) technique helps in decision-making by referencing past similar drilling situations. It is used for well planning, trajectory design, and troubleshooting, allowing the system to recommend solutions based on previously successful strategies. *CBR* systems grow more powerful over time as they accumulate more operational cases. This technique leverages historical case data for problem-solving and adapts solutions from similar past cases [39]. It is used to guide the selection of hole-cleaning procedures in unconsolidated formations, showing up to 80% match with expert decisions.

I.4.2.6 HYBRID TECHNIQUES

The hybrid techniques combine *ANNs*, fuzzy logic, *GAs* and *SVMs* to increase robustness and accuracy. As a result, these techniques have synergistic advantage of multiple *AI* methods for complex problem-solving and are used in offshore platform selection and drilling optimization [39].

I.4.3 AUTOMATED TOP DRIVE SYSTEMS

Automated top drive drilling systems represent a significant advancement in modern drilling technology, integrating robotics, real-time data analytics, and intelligent control to enhance efficiency and precision. These systems automate critical operations such as pipe handling, rotation, and torque management, reducing human intervention and minimizing errors. Equipped with advanced sensors and machine learning algorithms, they dynamically adjust drilling parameters (including *RPM*, weight-on-bit, and mud flow) to optimize performance and mitigate down-hole vibrations. By enabling a high performing connectivity with rig control systems and predictive maintenance tools, automated top drives improve drilling speed, safety, and reliability, making them indispensable in complex and high-risk drilling environments [40], [41].

Here are the key features of these intelligent systems:

• Adjust rotation speed (*RPM*), torque, and weight-on-bit (*WoB*) dynamically

• Use machine learning (*ML*) to predict and mitigate stick-slip and vibrations.

I.4.4 Adaptive Anti-Stick-Slip and Vibration Dampers

Modern drilling operations leverage adaptive anti-stick-slip and vibration dampers to mitigate destructive torsional and axial oscillations, enhancing drilling efficiency and tool longevity. These intelligent systems utilize real-time down-hole sensors and surface data to detect stick-slip, whirl, and other harmful vibrations, dynamically adjusting damping parameters through Model Predictive Control (*MPC*) or machine learning algorithms [40]. By autonomously modulating torque, *RPM*, and weight-on-bit, they suppress instabilities, reducing Non-Productive Time (*NPT*) and bit wear.

Integration with digital and cloud-based analytics further refines their reactivity, ensuring smoother drilling in challenging formations. These adaptive dampers represent a critical advancement in smart drilling, combining automation with precision for safer, faster, and more cost-effective operations [41].

These techniques include:

- Self-tuning algorithms to suppress harmful oscillations
- Active damping systems in smart Bottom Hole Assembly (*BHA*) [41].

That are characterized by:

- Autonomous adjustments which reduce human error
- Real-time optimization that maximizes *ROP* (Rate Of Penetration)
- And predictive maintenance that extends tool life.

Generally, these intelligent controllers represent the future of drilling systems, combining *IoT*, *AI*, and robotics for smarter, faster, and safer operations.

I.5 Control Techniques for Stick-Slip Oscillation Suppression

Stick-slip oscillations in drilling systems are a significant challenge, leading to equipment wear, reduced drilling efficiency, and potential failures. Over the past decade, various advanced control techniques have been developed to mitigate these vibrations. Here's an overview of the state-of-the-art methods:

Traditional Proportional-Integral-Derivative (*PID*) control has been applied to suppress stick-slip vibrations in drill strings. While effective in certain scenarios, the performance of *PID* controllers may be limited under varying operational conditions [42].

Fractional-Order *PID* (*FOPID*) controllers that incorporates fractional-order derivatives and integrals, provide better adaptability to the nonlinear and time-varying dynamics of drill strings, allowing for more precise damping of torsional vibrations. Studies have shown that *FOPID* controllers can effectively reduce stick-slip amplitude by optimizing both the controller gains and the fractional orders, leading to improved drilling stability and reduced wear. While *FOPID* offers theoretical advantages for SSO suppression, its practical adoption is hindered by computational demands, tuning complexity [43].

Fuzzy *PID* (That combines conventional *PID* with fuzzy logic to dynamically adjust gains based on real-time system behavior) and fuzzy tuned *FOPID* (That combines fuzzy adaptation with fractional-order tuning for better real-time performance) have been used to handle nonlinearities and uncertainties in drilling dynamics [44].

Linear Quadratic Regulator (*LQR*) control combined with *Luenberger* state observers is a model-based approach for mitigating stick-slip vibrations. While it offers strong theoretical performance, it has practical limitations in drilling applications [45].

Observer-Based Linear Quadratic Gaussian (*LQG*) controllers (combined with *Kalman* filter) have shown effectiveness in suppressing severe stick-slip vibrations. These controllers estimate immeasurable states, such as the drill bit's rotational velocity, using surface measurements like top drive current and rotational speed. Studies have demonstrated that observer-based LQG controllers can suppress high-frequency stick-slip vibrations within seconds, outperforming traditional H∞ controllers in terms of robustness and response time. The problem is these controllers are characterized by high computational complexity, difficulty in choosing weighting matrices and model dependency [45].

Sliding Mode Control (*SMC*) techniques are robust control methods that have been extensively applied to drilling systems. But their several variants (that include adaptive *SMC*, Hybrid back-stepping *SMC*, super-twisting *SMC*) real-world application in SSO suppression is hindered by chattering, tuning difficulties, measurement delays, and actuator constraints [46], [47].

While neural and neuro-fuzzy techniques offer adaptive, model-free SSO suppression, their data dependency, computational cost, and lack of stability guarantees limit real-world drilling applications. Hybrid methods (such as *ANN* + robust control) may be more viable [40], [44].

I.6 CONCLUSION

In this chapter, we explored the historical evolution, modeling, and control strategies of drilling systems, highlighting their critical role in modern oil and gas operations. From the earliest percussion drilling techniques to today's *AI*-driven and automated systems, the drilling industry has undergone remarkable technological advancements.

The modeling of the drill string, particularly through methods like *FEM* analysis, lumped parameter models, and advanced *nDOF* dynamic representations, provides essential insights into complex down-hole behaviors such as stick-slip, bit-bounce and lateral whirl. These models are fundamental for optimizing drilling performance, minimizing risks and ensuring operational safety.

Furthermore, the integration of *AI* techniques into drilling systems control has opened new horizons for real-time decision-making, predictive maintenance, and enhanced drilling efficiency. Despite some limitations, these techniques (such as neural networks, fuzzy logic and hybrid systems) have demonstrated strong potential in addressing the industry's most challenging problems.

Continuous innovation in drilling systems modeling and intelligent control is crucial to meet the future demands of safer, faster and more sustainable drilling operations.

Chapter II

Drilling Systems: Modeling & Control

II.1 INTRODUCTION

The drilling-string system is a critical component in oil and gas well operations, responsible for transmitting mechanical energy from the surface to the drill bit at the bottom of the wellbore. Due to the complex dynamic behaviors such as stick-slip vibrations, torsional instability, and down-hole disturbances, accurate modeling and effective control of the drilling-string system are essential for safe, efficient, and cost-effective drilling.

This chapter focuses on modeling and intelligent control of the drilling-string system, aiming to capture the nonlinear dynamics through mathematical models. Furthermore, intelligent control techniques are explored to enhance system stability, mitigate vibrations, and improve drilling performance under varying down-hole conditions. The integration of intelligent control provides a robust framework to handle uncertainties and real-time variations in drilling environments, contributing to smarter and more automated drilling operations.

II.2 DRILL STRING MODELING

Drill string modeling based on multi-degree-of-freedom (multi-*DOF*) dynamics provides a powerful and accurate framework for analyzing and mitigating complex down-hole vibrations. Unlike simplified low-order models, multi-*DOF* formulations capture the coupled interactions between torsional, axial, lateral, and bit-rock dynamics, enabling high-fidelity simulations essential for modern model-based control systems. These models serve as the foundation for predictive control, adaptive damping, and real-time optimization, ensuring stability and efficiency in drilling operations.

Stick-slip vibrations are a self-excited torsional instability but are strongly influenced by axial and lateral dynamics, as well as bit-rock interaction. A 4-*DOF* model is particularly effective for stick-slip control because it incorporates:

- Torsional dynamics that governs stick-slip oscillations and torque fluctuations.
- Axial dynamics that captures Weight-On-Bit (*WoB*) variations and bit bounce effects that interact with torsional vibrations.
- Lateral vibrations that accounts for whirl and bending stresses that can provoke stick-slip severity.
- Bit-rock interaction that models cutting forces and frictional effects that drive instability.

By considering these four coupled degrees of freedom, the model accurately replicates real-world drill string behavior, allowing controllers to:

- Predict and preemptively dampen stick-slip before it destabilizes the system.
- Optimize control gains for torsional-axial-lateral coupling, improving suppression performance.
- Enhance observer-based techniques (such as *Luenberger* observer) for real-time state estimation.

Thus, a 4-*DOF* drill string model is not just a theoretical improvement; it is a practical necessity for developing high-performance stick-slip control systems in modern drilling automation.

In this section, we will introduce the multi-*DOF* model of the drilling system and its simplified 4-*DOF* variant.

II.2.1 Multi-Degree of Freedom Torsional Model of a Drill String

A multi-*DOF* torsional model represents the complex dynamics of the drill string by considering multiple interconnected elements. While this approach captures detailed vibration behavior, it can be computationally intensive. In this study, a simplified 4-*DOF* torsional model is and control (see figure II.1).

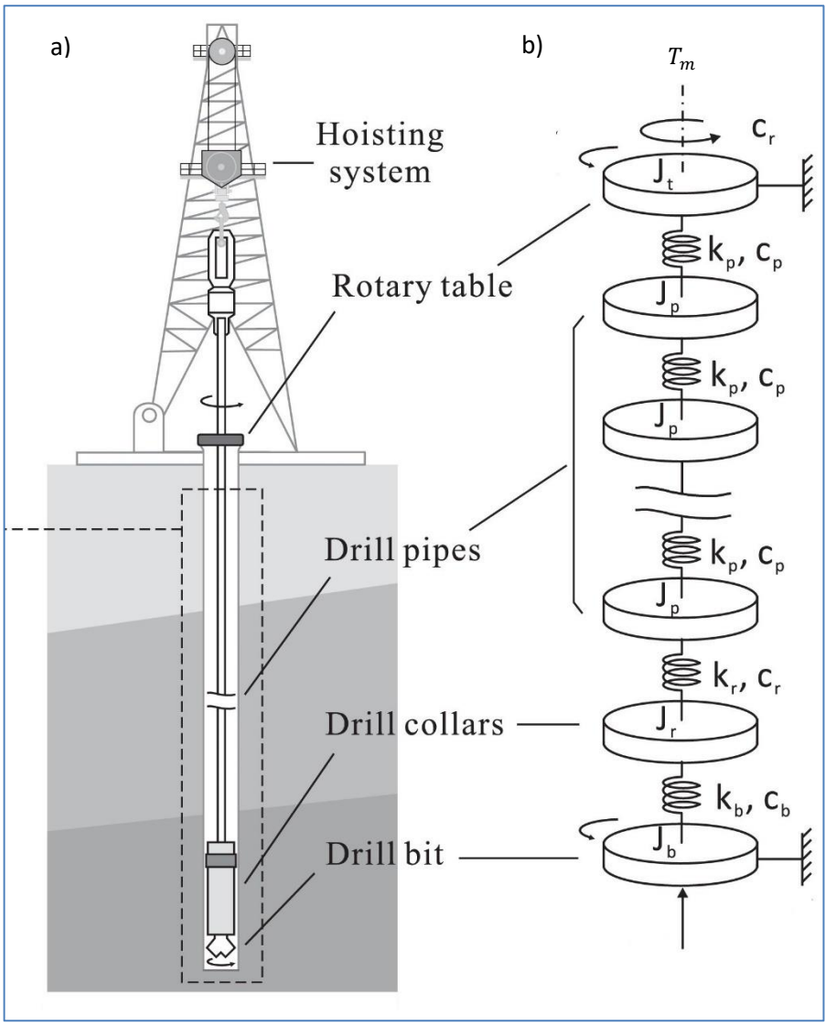

Figure II.1 a) An oil well drilling rig, b) A multi-*DOF* torsional model of the drill-string [48]

A multi-Degree Of Freedom (multi-*DOF*) torsional model of a drill string provides a more realistic and detailed representation of the complex dynamics that occur during drilling operations. Such a model considers various interconnected components including the rotary table, which drives the rotation; the drill pipes, which transmit torque and axial force; the drill collar, which provides additional weight and stiffness; and the drill bit, which interacts directly with the rock formation. Each of these components contributes to the system's dynamic behavior, and they are represented as discrete masses and inertias connected by torsional and axial stiffness and damping elements.

In an *n-DOF* system, the dynamics are typically governed by a set of coupled second-order differential equations. The general form of the motion equation for such a system is [49]:

$$J\ddot{\theta} + (C_1 + C_2)\dot{\theta} + K\theta = S_r T_r + S_b T_{ob} \quad \text{(II.1)}$$

Where:

$\theta = [\theta_r, \theta_{p1}, \ldots, \theta_{p(n-3)}, \theta_c, \theta_b]^T$ is a vector of '*n*' angular positions of the rotary table, the *n*-3 drill pipes, the drill collar and the drill bit respectively;

$S_r = [1, 0, \ldots, 0]^T$

$S_b = [0, 0, \ldots, -1]^T$

$J = diag\{J_r, J_{p1}, \ldots, J_{p(n-3)}, J_c, J_b\}$ is a diagonal matrix of the drilling system '*n*' elements: the rotary table, the *n*-3 drill pipes, the drill collar and the drill bit respectively;

$C_1 = diag\{d_r, d_{p1}, \ldots, d_{p(n-3)}, d_c, d_b\}$ is a diagonal matrix of the local damping factors of the '*n*' same elements of the drilling system;

T_r is the input torque generated by the top drive motor

T_{ob} is the friction torque resulted from bit-rock interaction

C_2 and *K* are mutual damping and torsional stiffness matrices given by:

$$C_2 = \begin{bmatrix} c_p & -c_p & 0 & 0 & \cdots & 0 & 0 & 0 & 0 \\ -c_p & 2c_p & -c_p & 0 & \cdots & 0 & 0 & 0 & 0 \\ 0 & c_p & 2c_p & -c_p & \cdots & 0 & 0 & 0 & 0 \\ \cdots & \cdots & \cdots & \cdots & \cdots & \cdots & \cdots & \cdots & \cdots \\ 0 & 0 & 0 & 0 & \cdots & -c_p & c_p + c_c & -c_c & 0 \\ 0 & 0 & 0 & 0 & \cdots & 0 & -c_c & c_c + c_b & -c_b \\ 0 & 0 & 0 & 0 & \cdots & 0 & 0 & -c_b & c_b \end{bmatrix} \quad \text{(II.2)}$$

$$K = \begin{bmatrix} k_p & -k_p & 0 & 0 & \cdots & 0 & 0 & 0 & 0 \\ -k_p & 2k_p & -k_p & 0 & \cdots & 0 & 0 & 0 & 0 \\ 0 & k_p & 2k_p & -k_p & \cdots & 0 & 0 & 0 & 0 \\ \cdots & \cdots & \cdots & \cdots & \cdots & \cdots & \cdots & \cdots & \cdots \\ 0 & 0 & 0 & 0 & \cdots & -k_p & k_p + k_c & -k_c & 0 \\ 0 & 0 & 0 & 0 & \cdots & 0 & -k_c & k_c + k_b & -k_b \\ 0 & 0 & 0 & 0 & \cdots & 0 & 0 & -k_b & k_b \end{bmatrix} \quad \text{(II.3)}$$

With: $C_{p,\,c,\,b}$ and $k_{p,\,c,b}$ specific values of damping and stiffness matrices elements corresponding to pipes, drill collar and drill bit respectively.

In order to facilitate analytical studies and controller synthesis, the drill string dynamic torsional model introduced in equation (II.1) is transformed into a standard state-space representation. This transformation enables the use of advanced control techniques such as optimal control and observer-based design.

To achieve this, we define a state vector $x(t)$ that captures both the angular velocities and relative angular displacements of the various elements along the drill string. Specifically, the state vector is constructed as follows [49]:

$$x = [\,\dot{\theta}_r\,,\ \dot{\theta}_{p1}, \dots,\ \dot{\theta}_{p(n-3)},\ \dot{\theta}_c,\ \dot{\theta}_b,\ \theta_{p1} - \theta_r,\ \theta_{p2} - \theta_{p1}, \dots,\ \theta_{p(n-3)} - \theta_{p(n-2)}\,,\ \theta_c - \theta_{p(n-3)},\ \theta_b - \theta_c\,]^T$$

This definition leads to a state-space model of the form:

$$\begin{cases} \dot{x}(t) = Ax(t) + Bu(t) + B_1 d(t) \\ y(t) = Cx(t) \end{cases} \tag{II.4}$$

Where:

$u(t)$ is the control input

$d(t)$ is the disturbance

A, B, B_1, C are the system matrices derived from mechanical and structural parameters of the drill string. These matrices are defined as follows [49]:

$$A = \begin{bmatrix} -J^{-1}(C_1 + C_2) & J^{-1}a_1 \\ a_2 & O_{n-1\times n-1} \end{bmatrix}$$

$$a_1 = \begin{bmatrix} -k_p & 0 & \cdots & 0 \\ k_p & -k_p & \cdots & 0 \\ \vdots & \ddots & \ddots & \vdots \\ 0 & \cdots & k_r & -k_b \\ 0 & \cdots & 0 & k_b \end{bmatrix}$$

$$a_2 = \begin{bmatrix} 1 & -1 & 0 & \cdots & 0 \\ 0 & \ddots & \ddots & \ddots & 0 \\ \vdots & \ddots & \ddots & \ddots & 0 \\ 0 & \cdots & 0 & 1 & -1 \end{bmatrix}$$

$$B = \begin{bmatrix} J^{-1}S_r \\ \boldsymbol{O}_{n-1\times 1} \end{bmatrix}$$

$$B_1 = \begin{bmatrix} J^{-1}S_b \\ \boldsymbol{O}_{n-1\times 1} \end{bmatrix}$$

$$C = \begin{bmatrix} 1 \\ \boldsymbol{O}_{2n-2\times 1} \end{bmatrix}^T$$

In this context, $'\boldsymbol{O}'$ is a zero matrix of appropriate dimensions. As indicated by Equation (II.4), the resulting state-space model has an order of $2n$, reflecting both the angular velocities and relative angular displacements of the system components.

In practical drill string systems, the number of discrete elements n can become very large, theoretically approaching infinity, due to the distributed and continuous nature of the physical structure. Therefore, adopting a multi-Degree Of Freedom (multi-*DOF*) torsional model is essential to accurately capture the complex torsional dynamics and behavior of the drill string in realistic operating conditions.

II.2.2 Four-Degree of Freedom Torsional Model of a Drill String

A 4-*DOF* torsional vibration model captures the rotational dynamics of a drilling system by representing the twisting motions of four key components: the rotary table (surface drive), drill pipe (flexible torque transmitter), drill collar (stiff, heavy section), and drill bit (cutting tool prone to stick-slip), see figure IV.2. This lumped-parameter model couples inertias, stiffness, and damping factors to analyze torsional waves, resonance, and stick-slip instability, it is critical for optimizing drilling efficiency and preventing tool damage. The governing equations describe how torque propagates down the string, with nonlinear bit-rock interaction often triggering harmful oscillations.

This reduced-order model is particularly useful for studying vibration phenomena in drilling systems while maintaining a manageable computational load. Each degree of freedom is associated with a corresponding displacement coordinate, and the system's dynamics can be described using coupled second-order differential equations that include inertia, damping, and stiffness components. These equations reflect the interaction between the different parts of the drill string such as the rotary table, drill pipes, drill collar, and drill bit. This model account for both internal structural characteristics and external forces, including bit-rock interaction and damping from the surrounding drilling fluid.

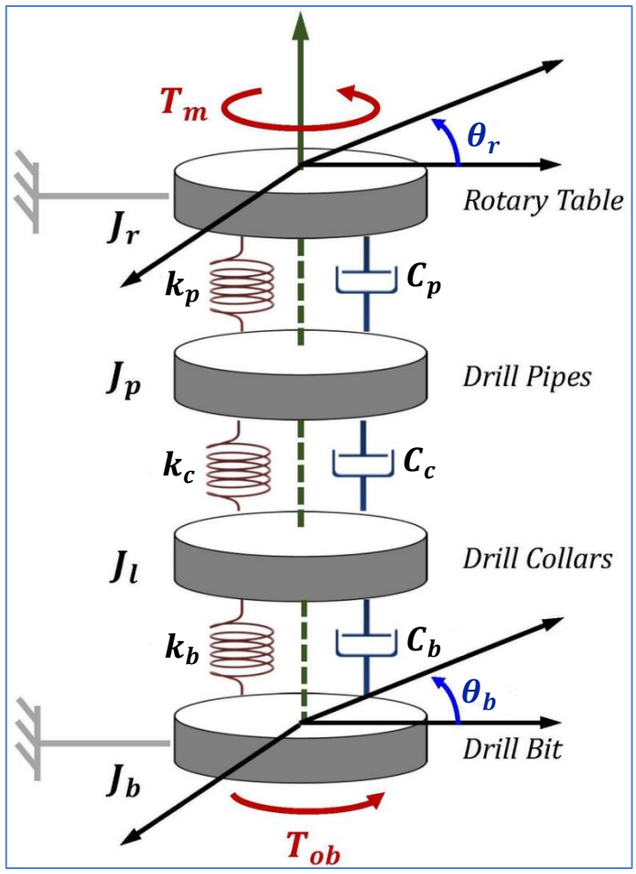

Figure II.2 A 4-*DOF* torsional model of the drill-string [50]

The system presented in Figure II.2, can be modeled as follows [50]:

$$\begin{cases} J_r\ddot{\theta}_r + c_p(\dot{\theta}_r - \dot{\theta}_p) + k_p(\theta_r - \theta_p) + c_r\dot{\theta}_r = T_m \\ J_p\ddot{\theta}_p - c_p(\dot{\theta}_r - \dot{\theta}_p) - k_p(\theta_r - \theta_p) + c_c(\dot{\theta}_p - \dot{\theta}_c) + k_c(\theta_p - \theta_c) = 0 \\ J_c\ddot{\theta}_c - c_c(\dot{\theta}_p - \dot{\theta}_c) - k_c(\theta_p - \theta_c) + c_b(\dot{\theta}_c - \dot{\theta}_b) + k_b(\theta_c - \theta_b) = 0 \\ J_b\ddot{\theta}_b - c_b(\dot{\theta}_c - \dot{\theta}_b) - k_b(\theta_c - \theta_b) + T_{ob} = 0 \end{cases} \quad \text{(II.5)}$$

Where:

$\theta_{(r,p,c,b)}$ are the angular displacements of the rotary table, the drill-pipe, the drill collar and the bit respectively.

$\dot{\theta}_{(r,p,c,b)}$ are the angular velocities of the rotary table, the drill-pipe, the drill collar and the bit respectively.

$\ddot{\theta}_{(r,p,c,b)}$ are the angular accelerations of the rotary table, the drill-pipe, the drill collar and the bit respectively.

$J_{(r,p,c,b)}$ are inertias of the rotary table, the drill-pipe, the drill collar and the bit respectively.

$c_{(r,p,c,b)}$ are the torsional damping coefficients of the rotary table, the drill-pipe, the drill collar and the bit respectively.

$k_{(p,c,b)}$ are the torsional stiffness coefficients at the drill-pipe, the drill-collar and the bit, respectively.

T_m is the input torque which is the drive torque produced by the driving system at the rotary table surface.

T_{ob} is the 'Torque On Bit' it represents the total reactive torque acting on the drill bit.

The number of the state variables depends on the system's degrees of freedom (*DOF*) '*n*' or the dimension of the torsional model. It can be shown that we have (2*n*−1) variables. In the case of a 4-*DOF* drilling system torsional model, the state vector consists of 7 elements, as shown below [50]:

$$x = \begin{pmatrix} x_1 \\ x_2 \\ x_3 \\ x_4 \\ x_5 \\ x_6 \\ x_7 \end{pmatrix} \quad \text{(II.6)}$$

Where:

$$\begin{cases} x_1 = \dot{\theta}_r \\ x_2 = \theta_r - \theta_p \\ x_3 = \dot{\theta}_p \\ x_4 = \theta_p - \theta_c \\ x_5 = \dot{\theta}_c \\ x_6 = \theta_c - \theta_b \\ x_7 = \dot{\theta}_b \end{cases} \quad \text{(II.7)}$$

Based on equations (II.5) and (II.7), one can write the following set of state equations:

$$\begin{cases} \dot{x}_1 = -\frac{c_p+c_r}{J_r}x_1 - \frac{k_p}{J_r}x_2 + \frac{c_p}{J_r}x_3 + \frac{T_m}{J_r} \\ \dot{x}_2 = x_1 - x_3 \\ \dot{x}_3 = \frac{c_p}{J_p}x_1 + \frac{k_p}{J_p}x_2 + \frac{c_c+c_p}{J_p}x_3 - \frac{k_c}{J_p}x_4 + \frac{c_c}{J_p}x_5 \\ \dot{x}_4 = x_3 - x_5 \\ \dot{x}_5 = \frac{c_c}{J_c}x_3 + \frac{k_c}{J_c}x_4 + \frac{c_c+c_b}{J_c}x_5 - \frac{k_b}{J_c}x_6 + \frac{c_b}{J_c}x_7 \\ \dot{x}_6 = x_5 - x_7 \\ \dot{x}_7 = \frac{c_b}{J_b}x_5 + \frac{k_b}{J_b}x_6 - \frac{c_b-c_d}{J_b}x_7 + \frac{T_{ob}}{J_b} \end{cases} \quad \text{(II.8)}$$

The state space model of equation (II.8) is similar to (II.4) recalled hereafter:

$$\begin{cases} \dot{x}(t) = Ax(t) + Bu(t) + B_1 d(t) \\ y(t) = Cx(t) \end{cases} \quad \text{(II.9)}$$

Where:

$$A = \begin{bmatrix} -\frac{c_p+c_r}{J_r} & -\frac{k_p}{J_r} & \frac{c_p}{J_r} & 0 & 0 & 0 & 0 \\ 1 & 0 & -1 & 0 & 0 & 0 & 0 \\ \frac{c_p}{J_p} & \frac{k_p}{J_p} & \frac{c_c+c_p}{J_p} & -\frac{k_c}{J_{p_p}} & \frac{c_c}{J_p} & 0 & 0 \\ 0 & 1 & 0 & -1 & 0 & 0 & 0 \\ 0 & 0 & \frac{c_c}{J_c} & \frac{k_c}{J_c} & \frac{c_c+c_b}{J_c} & -\frac{k_b}{J_c} & \frac{c_b}{J_c} \\ 0 & 0 & 0 & 0 & 1 & 0 & -1 \\ 0 & 0 & 0 & 0 & \frac{c_b}{J_b} & \frac{k_b}{J_b} & -\frac{c_b-c_d}{J_b} \end{bmatrix} \quad \text{(II.10)}$$

$$B = \begin{bmatrix} \frac{1}{J_r} & 0 & 0 & 0 & 0 & 0 & 0 \end{bmatrix}^t$$

$$B_1 = \begin{bmatrix} 0 & 0 & 0 & 0 & 0 & 0 & -\frac{1}{J_b} \end{bmatrix}^t$$

$$C = [1 \quad 0 \quad 0 \quad 0 \quad 0 \quad 0 \quad 0]^t$$

Note that y (with $y = x_1$) represents the system output which is the measured rotary table speed at the surface. The control input u represents the applied driving torque ($u = T_m$) and the disturbance d is the torque on the bit ($d = T_{ob}$).

II.2.3 MODELING OF THE TORQUE ON BIT BEHAVIOR

The torque on the drill bit noted 'T_{ob}' is primarily caused by the torque needed to crush and cut rock along with friction from the Bottom Hole Assembly (*BHA*). The interaction between the drill bit and the rock formation excites stick-slip vibrations in the drill string. Therefore, modeling the torque on the bit is crucial for understanding the vibration mechanism. Indeed, several friction models have been proposed in previous works.

Here are two of the most used models [49]:

- ***The first model*** of the bit-rock interaction which is widely used for modeling the T_{ob} is based on '*Karnopp'* model which is given by:

$$T_{ob} = WoB \times R_b\left(\mu_{cb} + (\mu_{sb} - \mu_{cb})e^{-\gamma_b|\dot{\theta}_b|}\right)sgn\left(\dot{\theta}_b\right) \quad \text{(II.11)}$$

Where:

WoB and R_b are the weight on the bit and the bit radius (positive values) respectively.

μ_{cb}, μ_{sb} and γ_b are the static and *Coulomb* friction coefficients associated with J_b , which parameterize the friction curve ($0 < \mu_{cb} < 1$, $0 < \mu_{sb} < 1$, $0 < \gamma_b < 1$).

- ***The second model*** of the resulted torque from bit–rock contact is expressed as a variation of the *Stribeck* friction added to the dry friction model. The dry friction model when $\dot{\theta}_b = 0$, is approximated by a combination of a switch model and another model in which a zero-velocity band is introduced (*Karnopp*'s model). This model is defined as follows [49]:

$$T_{ob}(\dot{\theta}_b) = \begin{cases} T_{obe}(\dot{\theta}_b) & if \ |\dot{\theta}_b| < \beta, \ |T_{obe}| \leq T_{obs} \\ T_{obs} sgn(T_{obe}(\dot{\theta}_b)) & if \ |\dot{\theta}_b| < \beta, \ |T_{obe}| > T_{obs} \\ T_{obb} sgn(\dot{\theta}_b) & if \ |\dot{\theta}_b| \geq \beta \end{cases} \quad \text{(II.12)}$$

Where:

$\beta > 0$ specifies a small enough neighborhood of $\dot{\theta}_b = 0$;

T_{obe} is the reaction torque that is the torque that the static friction torque T_{obs} must overcome so that the bit moves;

And $T_{obs} = \mu_{sb} WoB \times R_b$, with $R_b > 0$ the bit radius.

Moreover, the function $T_{obb}(\dot{\theta}_b)$ is given by:

$$T_{obb}(\dot{\theta}_b) = \mu_b(\dot{\theta}_b) \times WoB \times R_b \quad \text{(II.13)}$$

Where $\mu_b(\dot{\theta}_b)$ is the bit dry friction coefficient, that it is defined as follows:

$$\mu_b(\dot{\theta}_b) = \left(\mu_{cb} + (\mu_{sb} - \mu_{cb}) e^{-\gamma_b |\dot{\theta}_b|}\right) \quad \text{(II.14)}$$

II.3 DRILL STRING CONTROL STRATEGY FOR STICK-SLIP VIBRATION MITIGATION

The suppression of stick-slip vibrations in a drill string is tackled by framing it as a bit-speed tracking control problem, aiming to ensure the drill bit rotates at a desired speed despite disturbances. Due to the lack of real-time down-hole measurements, only surface data such as rotary table speed and torque can be used. To address this limitation, an observer-based control system is introduced. It includes a state observer that estimates the unmeasured internal states of the system, such as bit speed, from surface-level inputs. These estimates feed into a tracking controller designed to minimize the error between the desired and estimated bit speed. The system is further enhanced to ensure zero steady-state error, guaranteeing accurate long-term performance even with model uncertainties and disturbances. This integrated control strategy offers a practical and robust solution for real-time suppression of stick-slip using only surface measurements (see figure II.3).

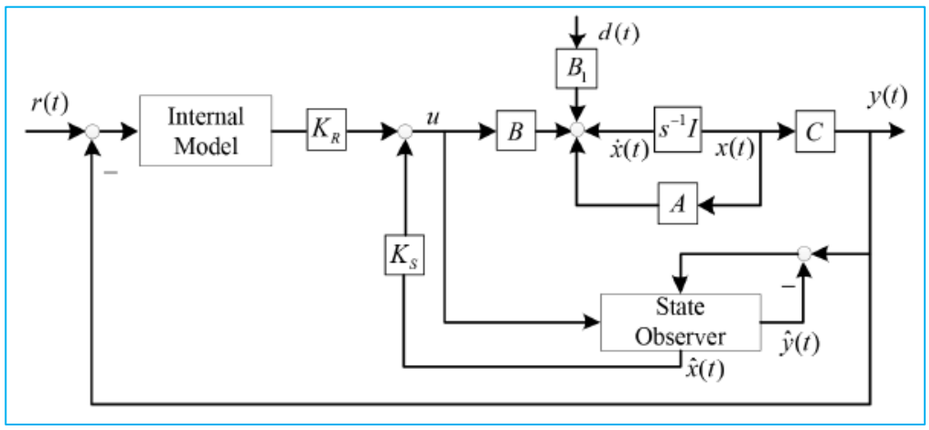

Figure II.3 Structure of the drill string control system [49]

II.3.1 STATE SPACE OBSERVER

In control systems, an observer is a mathematical algorithm or model used to estimate the internal (unmeasured) states of a dynamic system based on available measurements (outputs) and input signals. Since it is often impossible or impractical to measure all the necessary internal variables of a system especially in complex or remote environments like down-hole drilling, observers play a crucial role in enabling feedback control when full state information is not directly accessible.

An observer reconstructs or estimates the unmeasured state vector $x(t)$ using known inputs $u(t)$ and outputs $y(t)$.

Various types of observers are employed to estimate the internal states of a system when direct measurement is impractical. The *Luenberger* observer is a deterministic state observer that uses output feedback to asymptotically converge to the true state, provided the system is observable. The Sliding Mode Observer (*SMO*) is robust to uncertainties and disturbances but may introduce chattering. The *Kalman* filter is optimal for stochastic systems with *Gaussian* noise, minimizing estimation error covariance. Non-Linear Observers (*NLO*), such as high-gain or extended observers, handle nonlinear dynamics but may require complex tuning.

The *Luenberger* observer is often preferred for linear systems due to its simplicity, guaranteed convergence under observability conditions, and ease of implementation compared to more complex observers like the *Kalman* filter or *SMO*, which are better suited for noisy or uncertain environments. Its deterministic nature and straightforward design make it a reliable choice for many engineering applications. It is one of the most commonly used observers and it is defined by:

$$\begin{aligned} \dot{\hat{x}}(t) &= A\hat{x}(t) + Bu(t) + L(y(t) - \hat{y}(t)) \\ \hat{y}(t) &= C\hat{x}(t) \end{aligned} \tag{II.15}$$

Where:

$\hat{x}(t)$ is the estimated state vector

$\hat{y}(t)$ is the estimated output

L is the observer gain matrix.

In drilling systems, observers are used to estimate critical downhole parameters like bit speed, torque, or vibrations, which cannot be directly measured in real time as it has mentioned previously. These estimates are essential for implementing control strategies such as bit-speed tracking control, enabling the suppression of undesirable behaviors like stick-slip vibrations, even when only surface measurements are available.

II.3.2 *LQR* Optimal Control

The Linear Quadratic Regulator (*LQR*) is an optimal control strategy used to determine the best state-feedback control law for linear dynamic systems. It minimizes a quadratic cost function that balances system performance (how close the states are to desired values) and control effort (how much energy is used in the control input). *LQR* provides a feedback gain matrix that ensures stability, optimal performance, and robustness in the presence of small disturbances.

The goal of *LQR* is to find an *LTI* system control input $u(t)$ that minimizes a quadratic cost function [51]:

$$J = \frac{1}{2}\int_0^{\infty}(x^T(t)Qx(t) + u^T(t)Ru(t))dt \quad \text{(II.16)}$$

Where:

Q is a positive semi-definite state cost matrix

R is a positive definite control cost matrix.

The task of the state regulator is to keep each component of the system state close to the desired state without consuming too much energy when the system state deviates from the equilibrium state for any reason.

Therefore, the control of the stick-slip vibration of the drill string system is mainly to enable the rotary table and the *BHA* to track the desired rotational speed in real time, and maintain a small torsion angle of the drill string, which is reflected in the performance index to reduce the angular velocity and angular displacement deviation of the rotary table as much as possible, and the required active control torque should be within the maximum power range of the rotary table driver.

In this case, the control input $u(t)$ is expressed as linear feedback of the state:

$$u(t) = -K_x x(t) \quad \text{(II.17)}$$

Where K_x is the feedback gain matrix, derived to optimize system performance.

It is obtained by solving the following Algebraic *Riccati* Equation (*ARE*) [51]:

$$A^T P + PA - PBR^{-1}B^T P + Q = 0 \quad \text{(II.18)}$$

Once the matrix P is computed, the optimal gain K is determined as follows:

$$K_x = R^{-1}B^T P \quad \text{(II.19)}$$

In many control applications, especially when we want to ensure zero steady-state error, we augment the original state vector $x(t)$ with additional variables (like integral of the error, or references). This gives an augmented state vector $\bar{x}(t)$. In this case:

$$u(t) = -\bar{K}_x \bar{x}(t) \quad \text{(II.20)}$$

Where:

$\bar{K}_x = [K_s\ K_R]$ and $\bar{x} = \begin{bmatrix} x(t) \\ x_R(t) \end{bmatrix}$

K_s is the gain of the state feedback

K_R is the gain of the internal model which is (in our case) an integrator action used to suppress the steady state error.

$\bar{x}(t)$ includes both the original state vector $x(t)$ and any added variables (the integral of the dynamic error on output in this case, see figure II.3).

The *LQR*, which is a widely used optimal control technique, offers several advantages. First, it provides a systematic approach to design state-feedback controllers by minimizing a quadratic cost function that balances state deviations and control effort, ensuring optimal performance. Second, *LQR* guarantees closed-loop stability for linear systems, assuming controllability and observability. Third, it handles multi-input multi-output (*MIMO*) systems efficiently, unlike many classical control methods. Additionally, *LQR* solutions are computationally efficient, relying on solving the algebraic *Riccati* equation, which ensures a globally optimal solution.

This method also allows for tuning flexibility through the weighting matrices, enabling designers to prioritize either state regulation or control energy minimization. Due to its robustness, optimality, and ease of implementation, *LQR* is widely applied in industrial automation.

II.3.3 INTERNAL MODEL

To achieve zero steady-state error in tracking the reference speed and rejecting persistent disturbances, the control strategy integrates an internal model of the reference signal into the closed-loop system. This approach is grounded in the internal model principle, which asserts that perfect tracking and disturbance rejection are only possible when the controller includes a dynamic model of the signals it aims to track. Mathematically, the internal model is described by the following dynamic system [51]:

$$\begin{cases} \dot{x}_c(t) = A_c x_c(t) + B_c e(t) \\ y_c(t) = C_c x_c(t) \end{cases} \quad \text{(II.21)}$$

Where:

$e(t)$ is the tracking dynamic error on the output expressed as $e(t) = r(t) - y(t)$, with $r(t)$ being the reference signal and $y(t)$ the plant output.

x_c is the internal model state

A_c, B_c and C_c are matrices defining the internal model dynamics.

To combine the plant and the internal model into a single unified system, an augmented state vector is defined as follows:

$$\bar{x}(t) = \begin{bmatrix} x(t) \\ x_c(t) \end{bmatrix}$$

The augmented system can then be expressed in the following form:

$$\dot{\bar{x}}(t) = \bar{A}\bar{x}(t) + \bar{B}u(t) + \bar{B}_1 d(t)$$

$$\dot{\bar{x}}(t) = \begin{pmatrix} A & 0 \\ -B_c C & B_c \end{pmatrix} \bar{x}(t) + \begin{pmatrix} B \\ 0 \end{pmatrix} u(t) + \begin{pmatrix} B_1 \\ 0 \end{pmatrix} d(t) \quad \text{(II.22)}$$

This structure enables the controller to embed the dynamics of the reference or disturbance signal into the control law. When this augmented model is used in conjunction with an optimal control technique such as *LQR*, it allows for precise reference tracking and disturbance rejection, with guaranteed zero steady-state error in the presence of constant or predictable inputs.

II.3.4 WEIGHTING MATRICES TUNING AND CONTROL EFFECTIVENESS

The weighting matrices Q (state cost) and R (control cost) are critical in *LQR* design, as they determine the trade-off between state regulation and control effort. A larger Q penalizes state deviations more heavily, leading to faster convergence but potentially requiring higher control energy. Conversely, a larger R restricts control effort, improving energy efficiency but possibly slowing down the system response. Proper tuning ensures optimal performance that ensures balancing speed, overshoot, and actuator constraints. Poorly chosen weights can lead to instability or sluggish behavior, making systematic tuning methods essential for achieving desired dynamics.

To assess *LQR* performance, Mean Squared Error (*MSE*) or Integral Squared Error (*ISE*) is a common metric, quantifying the average squared deviation of states from equilibrium, reflecting regulation accuracy. Other key evaluation methods include settling time (speed of convergence), overshoot (peak deviation), and control effort (energy dissipation).

For robustness analysis, sensitivity to disturbances and stability margins (gain/phase) are examined. By combining *MSE* with these metrics, one can clearly judge control effectiveness, ensuring the *LQR* meets both transient and steady-state requirements while maintaining efficiency and robustness.

Several performance criteria can be used to evaluate and optimize system behavior. One of the most widely used is the Integral of Squared Error (ISE), which quantifies the accumulated squared tracking error over time. It is mathematically defined as follows [51]:

$$ISE = \int_0^\infty e^2(t)dt \tag{II.23}$$

The objective is typically to minimize this quantity to ensure that the error remains as small as possible during the system's operation. Other performance criteria consist of minimizing:

- Integral of Absolute Error (*IAE*): $\int_0^\infty |e(t)|dt$
- Integral of Time-weighted Absolute Error (*ITAE*): $\int_0^\infty t|e(t)|dt$
- Integral of Time-weighted Squared Error (*ITSE*): $\int_0^\infty te^2(t)dt$

In this work, an optimization procedure is proposed to fine-tune the Q & R matrices elements by optimizing an *MSE* criterion that evaluates the control effectiveness (see chapter IV).

II.4 CONCLUSION

This chapter has provided a thorough analysis of the modeling and control of a drilling-string system, which are central to efficient and safe oil and gas well operations. A multi-Degree Of Freedom (multi-*DOF*) modeling approach was adopted to realistically represent the complex dynamics of the drill string torsional motion. The 4-*DOF* torsional model that offered a balance between computational feasibility and physical accuracy, enabling effective analysis of key vibrational behaviors, has been elaborated.

State-space formulations were developed to facilitate advanced control design, particularly under challenging conditions like stick-slip vibrations and uncertain down-hole environments. Two friction models for the torque on the bit (T_{ob}) the *Karnopp* and modified *Stribeck* models were presented to capture the nonlinear interactions between the drill bit and rock.

The chapter also introduced an intelligent control strategy dedicated to suppress stick-slip vibrations using only surface-level data. This was achieved through a *Luenberger* observer-based design that estimates unmeasured states. A Linear Quadratic Regulator (*LQR*) combined with an internal model structure has been implemented to ensure an optimal bit-speed tracking and zero steady-state error. Performance metrics like *MSE* were discussed to optimize the weighting matrices and evaluate control effectiveness.

Overall, the integration of modeling, state estimation, and optimal control strategies provides a robust framework for improving drilling performance, enabling smarter and more autonomous drilling operations in complex and uncertain environments.

Chapter III

Case Study of an LQR-based Control of a 4-DOF Drilling System

III.1 INTRODUCTION

Drilling systems are subject to self-excited torsional vibrations, particularly stick-slip oscillations, which reduce drilling efficiency, accelerate tool wear, and increase operational risks. In the previous chapter, a 4-*DOF* lumped-parameter model of a drill string was developed, and an *LQR*-based control strategy with integral action was designed to regulate the rotary table speed while suppressing stick-slip oscillations. A *Luenberger* observer was further implemented to estimate unmeasured states for feedback.

To validate the theoretical framework, this chapter presents a practical case study applying the proposed controller to a realistic drilling system. The objectives of this chapter are threefold:

- Present the case study system, including its physical parameters and operational conditions.
- Implement the control architecture (*LQR* + integral action + observer) and adapt it to the case study under *MATLAB*.
- Evaluate performance through simulations, comparing open-loop and closed-loop behavior to demonstrate stick-slip mitigation.

This chapter is structured as follows: First, the drilling system configuration and parameters are detailed. Next, the control implementation is discussed, including tuning adjustments. Simulation results are then analyzed for both open and closed-loop scenarios, followed by a critical discussion of limitations and trade-offs. The aim of this chapter is to demonstrate the feasibility and efficiency of the investigated control strategy under realistic conditions, paving the way for future improvements and/or experimental or field validation.

III.2 CASE STUDY SYSTEM DESCRIPTION

To evaluate the effectiveness of the proposed control strategy, a representative case study of a vertical oilwell drilling system is considered. The configuration and parameters are taken from the validated framework presented in [48], providing a realistic benchmark for simulation and control performance evaluation using only top-side measurements.

III.2.1 DRILLING SYSTEM CONFIGURATION

The system is modeled using a 4-*DOF* lumped-parameter structure that captures the essential torsional dynamics of key components: the rotary table, drill pipe, drill collar, and drill bit (as shown in Chapter II, Figure II.2.). This model incorporates both structural dynamics and nonlinear bit-rock interaction effects to reflect real-world stick-slip phenomena. Each segment of the string (rotary table, drill pipe, collar, bit) is modeled by its torsional inertia, damping, and stiffness. The rotary table applies a controlled torque, while the bit interacts nonlinearly with the rock formation via the bit-rock friction model defined in Equations (II.11)–(II.14).

III.2.2 PARAMETERS OF THE 4-*DOF* TORSIONAL MODEL

The physical and mechanical parameters used in the simulation of the 4-*DOF* torsional drill string model are summarized in Table III.1. These values are chosen based on representative field data and validated literature to ensure realistic modeling of the drilling process.

Table III.1 Parameters of the 4-*DOF* torsional drill string model [48]

Parameter	Value	Unit	Parameter	Value	Unit	Parameter	Value	Unit
J_r	930	kg.m²	J_p	2782.25	kg·m²	J_c	750	kg·m²
J_b	471.97	kg.m²	k_p	698.06	Nm/rad	k_c	1080	Nm/rad
k_b	907.48	Nm/rad	d_r	425	Nms/rad	d_p	0	Nms/rad
d_c	0	Nms/rad	d_b	50	Nms/rad	c_p	139.61	Nms/rad
c_c	190	Nms/rad	c_b	181.49	Nms/rad	WoB	97347	N
R_b	0.1556	m	μ_{cb}	0.5	-	μ_{sb}	0.8	-
β	10^{-6}	rad/s	γ_b	0.9	s/rad	v_f	1	-

This table includes inertias of the drill string components, torsional stiffness and damping factors between sections, and key friction-related parameters influencing bit-rock interaction. The nonlinear friction behavior at the bit is modeled using *Karnopp* model and *Stribeck* approximation to accurately capture stick-slip effects, *Coulomb* friction, and viscous damping (see Equations II.11 – II.14).

III.3 *LQR* CONTROL & OBSERVER IMPLEMENTATION AND PARAMETERS TUNING

The suppression of stick-slip vibrations in a drill string is tackled by framing it as a bit-speed tracking control problem, aiming to ensure the drill bit rotates at a desired speed despite disturbances. Due to the lack of real-time downhole measurements, only surface data such as rotary table speed and torque can be used. To address this limitation, an observer-based control system is introduced. It includes a *Luenberger* state observer that estimates the unmeasured internal states of the system, such as bit speed, from surface-level inputs. These estimates feed into a tracking controller designed to minimize the error between the desired and estimated bit speed. The system is further enhanced (with an internal model generating an integral action) to ensure zero steady-state error, guaranteeing accurate long-term performance even with model uncertainties and disturbances (see Figure III.1 which is the Figure II.3 reproduced hereafter as a reminder).

In control systems, an observer is a mathematical algorithm or model used to estimate the internal (unmeasured) states of a dynamic system based on available measurements (outputs) and input signals. Since it is often impossible or impractical to measure all the necessary internal variables of a system especially in complex or remote environments like downhole drilling, observers play a crucial role in enabling feedback control when full state information is not directly accessible.

The system structure shown in Figure III.1, includes the drill string dynamic model, the internal model (integrator acting on rotary table speed error), state feedback and state observer, respectively. The internal model state equation is given by [48]:

$$\begin{cases} \dot{x}_c = A_c x_c(t) + B_c e(t) \\ y_c(t) = C_c x_c(t) \end{cases}$$

Where the input is the dynamic error on rotary speed table: $e(t)=r(t)-y(t)$ and: Ac=0, B_c=1 and C_c=1.

The augmented state ($\overline{x}(t) = [x(t)\ x_c(t)]^T$) representation of the plant associated to the internal model is given by:

$$\dot{\bar{x}}(t) = \overline{A}\,\bar{x}(t) + B\,\bar{u}(t) + \bar{B}_1 d(t)$$
$$= \begin{bmatrix} A & 0 \\ -B_c C & B_c \end{bmatrix} \bar{x}(t) + \begin{bmatrix} B \\ 0 \end{bmatrix} u(t) + \begin{bmatrix} B_1 \\ 0 \end{bmatrix} d(t)$$

And the control law is formulated by:

$$u(t) = -\overline{K}\bar{x}(t) = [-K_S\ K_R]\,\bar{x}(t)$$

Where K_S and K_R are the gains matrices of the state feedback and the internal model, respectively.

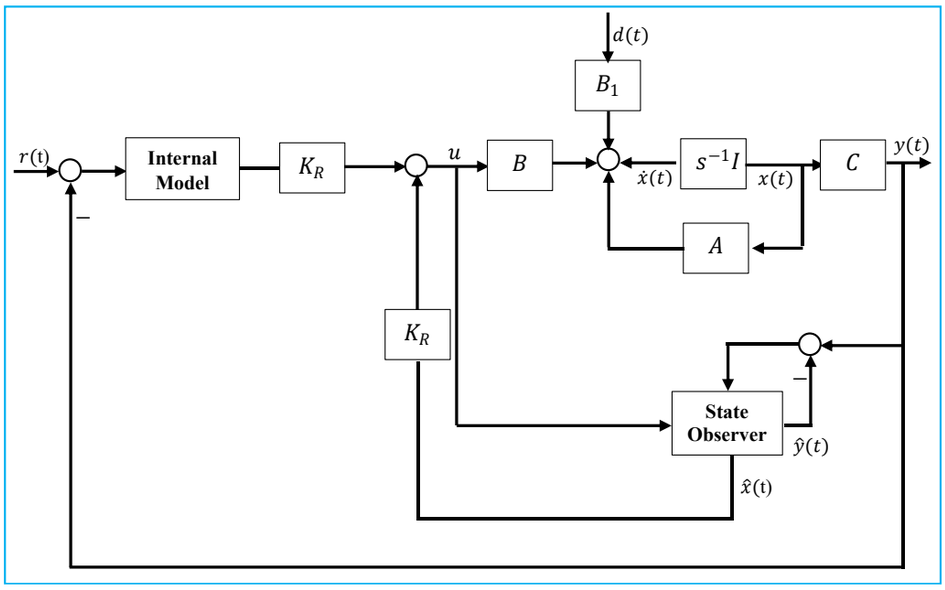

Figure III.1 Structure of the investigated drill string control system [48]

Elsewhere, in practical drilling process, only top measurement is available, which makes the control based on full state feedback impossible. Therefore, a full-dimensional state observer is used to estimate the state; it is governed by the following state equation [48]:

$$\begin{cases} \dot{\hat{x}}(t) = A\hat{x}(t) + Bu(t) + L\big(y(t) - \hat{y}(t)\big) \\ \hat{y}(t) = C\hat{x}(t) \end{cases}$$

Recall that:

$\hat{x}(t)$ is the estimated state vector

$\hat{x}(t)$ is the estimated output

L is the observer gain matrix.

Effective tuning of the controller and observer is critical for stabilizing the drilling system and ensuring accurate estimation of unmeasured states. We use a state-feedback control and a *Luenberger* observer, tuned using linear quadratic regulator optimal control algorithm preprogrammed under *MATLAB*, on the basis of chosen error weighting matrix and control weighting matrix [48].

III.3.1 *LQR* PARAMETERS TUNING

The controller is responsible for adjusting the surface torque to keep the drill bit rotating smoothly, even under harsh conditions (like friction at the rock). To do this effectively, its parameters must be tuned to balance three main goals:

- ***Good accuracy*** by tracking conveniently the desired speed at the bit
- ***Fast time settlement*** to reach the target quickly without large overshoots
- ***Stability*** to handle disturbances like stick-slip vibrations.

The controller was tuned using the *LQR* algorithm of *MATLAB* as mentioned earlier. This method automatically calculates controller gains by minimizing a cost function that balances:

- Tracking error (difference between desired and actual speed)
- Control effort (how hard the system works).

The weighting Q matrix that is used to prioritize critical state variables, like angular speed and torsional angle, has been conveniently tuned in [48] via trial-and-error method as follows:

$$Q = diag(1\ \ 1\ \ 1\ \ 10\ \ 1\ \ 1\ \ 1\ \ 1000) \tag{III.1}$$

Same thing for the control weight (R) that is used to penalize excessive torque changes, avoiding actuator saturation [48]:

$$R = 0.001 \tag{III.2}$$

As a consequence, the gain of state feedback and internal model are:

$$K_S = [735.3\ \ 2490.5\ \ 504.9\ \ 247.6\ \ 611.6\ \ 909.0\ \ 959.5]$$
$$K_R = 1000 \tag{III.3}$$

III.3.2 OBSERVER PARAMETERS TUNING

Since sensors at the bottom (bit) are not available, an observer is used to estimate those hidden states using only surface measurements.

In order to estimate the state of drill string dynamic, a set of poles determined also through trial and error in [48] has been adopted:

$$P = [-0.93 \quad -2 \pm 0{,}84i \quad -1.5 \pm 1i \quad -3 \pm 1.95i\ ] \tag{III.4}$$

Then, the pole placement algorithm of *MATLAB* has been used to determine the gain matrix state-feedback of the observer [48]:

$$L = [12.22\ \ 178.38\ \ -301.66\ \ -80.86\ \ -52.89\ \ -580.81\ \ 633.20]^T \tag{III.5}$$

III.4 SIMULATION RESULTS AND ANALYSIS

This section presents and analyzes the simulation results obtained using the 4-*DOF* torsional drill string model presented in Section III.2, and the observer-based tracking *LQR* controller designed and tuned as described in Section III.3. The primary objective of these simulations is to validate the effectiveness of this control strategy proposed in [48] in terms of suppressing stick-slip vibrations and to assess the performance of the state observer.

The analysis will first examine the open-loop behavior (in sticking, stick-slip and normal modes of operation) of the system to highlight the stick-slip problem, followed by an evaluation of the closed-loop system under control, including its robustness to disturbances.

III.4.1 Open-Loop System Behavior

The open-loop drill-string system shows unstable vibrations in stick-slip mode of operation. In fact, the rotary table and bit speeds are permanently oscillating around the reference speed due to frictional effects. This instability highlights the need for feedback control to ensure stable and efficient operation. Figure III.2 illustrates the open-loop dynamic behavior of the drill-string system by plotting the rotary table speed with the bit speed over time. The system exhibits clear stick-slip vibrations, characterized by periodic and irregular oscillations in the rotary table speed. These fluctuations result from the nonlinear frictional interactions between the drill bit and the rock formation, which lead to intermittent sticking and slipping phases. The oscillations of the actual speeds persist without damping, indicating poor dynamic performance and absence of corrective control. This behavior is typical in open-loop systems where no feedback mechanism is employed to regulate speed or suppress mechanical instabilities. The presence of sustained vibrations not only reduces drilling efficiency but can also lead to mechanical wear and structural fatigue in the drill-string components.

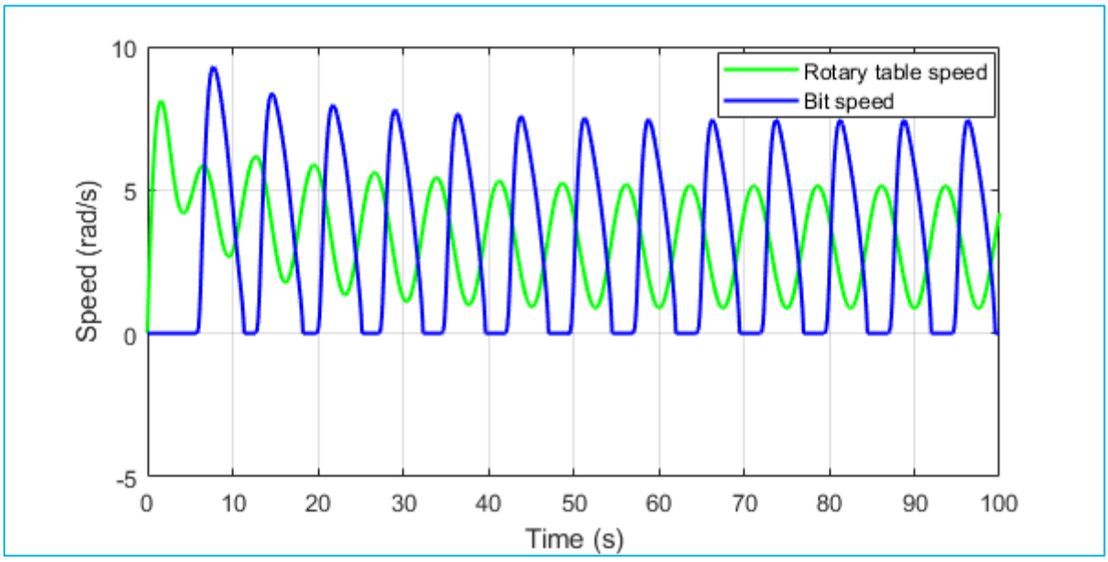

Figure III.2 Rotary table and bit speed vibration in stick-slip mode of operation of the drill string system

Figure III.3 illustrates the different modes of operation of the drill-string system in the plane (T_m & WoB). The diagram on the left (obtained via trial and error simulation tests) delineates three primary zones:

- Bit sticking area
- Stick-slip area
- And stable rotation area.

These regimes are mapped as a function of the control torque T_m and WoB, indicating that the system transitions between unstable and stable behaviors depend strongly on operating conditions, especially the control torque for a given WoB.

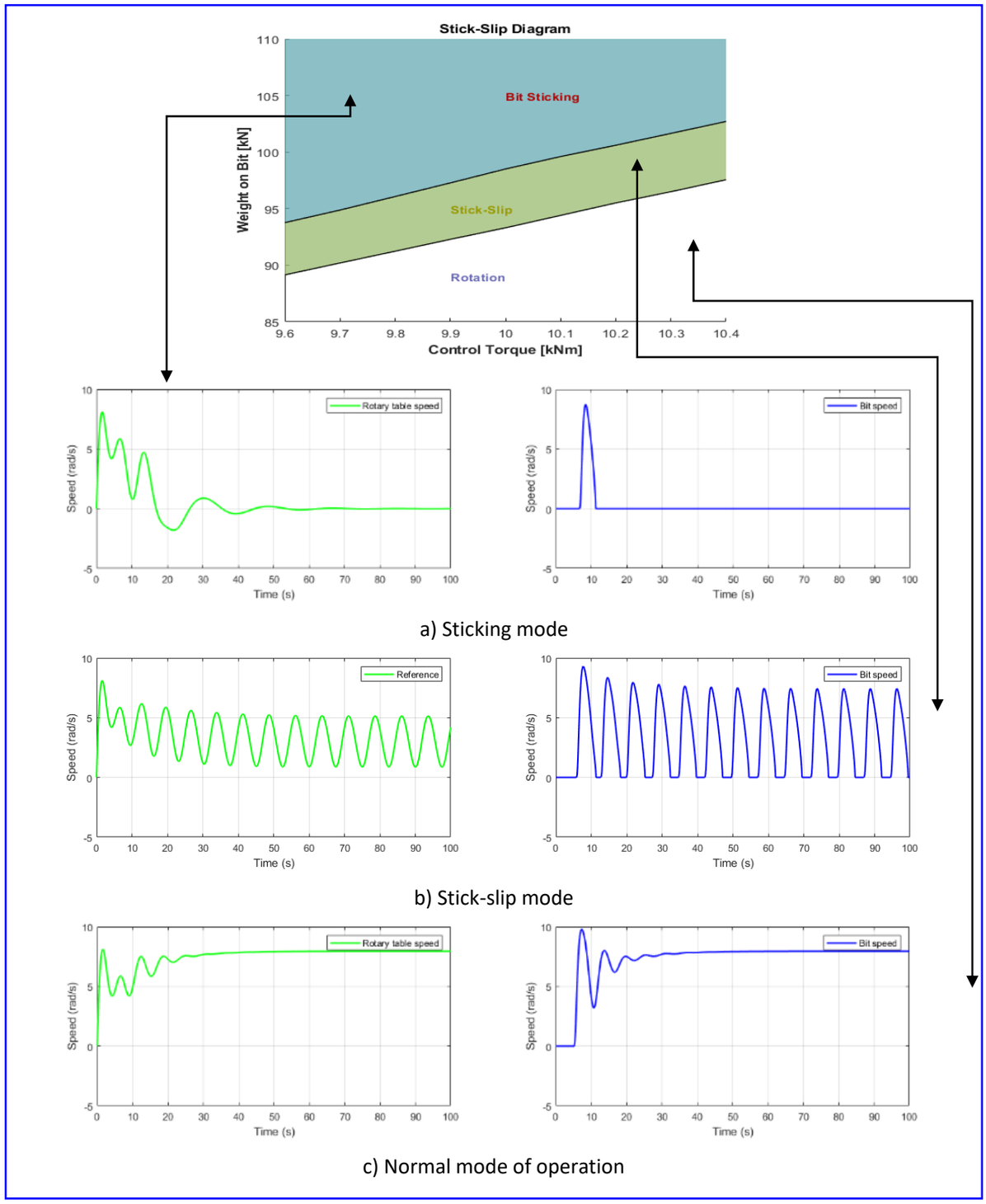

Figure III.3 Different operating modes of the drill-string system in the plan of (control torque T_m & *WoB*)

The plots on the right correspond to selected operating points in the three zones and show the system's time response under those conditions. In the bit sticking mode and stick-slip zone, the system exhibits pronounced oscillations and instability, confirming the presence of undesired dynamic effects. However, when the system operates within the stable rotation zone, achieved through appropriate combination of control torque and *WoB*, the response becomes smoother and more consistent. This figure emphasizes the critical impact of operating conditions on the drill-string dynamics and highlights the necessity of active control strategies to maintain the system within stable operating conditions and prevent performance degradation.

III.4.2 Closed-Loop System Behavior and Performance

This section evaluates the performance of the *LQR*-based controller in closed-loop operation, focusing on its ability to suppress torsional vibrations, track the desired speed, and maintain stability under variation of load conditions and changes in the *WoB*.

Figure III.4 illustrates the dynamic response of the drill string system under closed-loop control using *LQR*. The reference speed (ω_d=12 *rpm*) represents the desired setpoint that the *LQR* controller aims to track. Initially, both the rotary table speed and the drill bit speed increase toward the reference value, with noticeable oscillations in the bit speed caused by the torsional dynamics of the drill string. During this phase $t\epsilon$[0 50]s, the *WoB* is maintained at 97.347 kN. As time progresses, these oscillations are effectively damped by the *LQR* controller. At t = 50 seconds, the *WoB* has been increased to 110 kN, introducing a disturbance into the system. Despite this change, the system remains stable, and both speeds regain and track closely the reference speed. The zoomed-in section highlights minimal residual oscillations, demonstrating the robustness and effectiveness of the *LQR*-based control strategy in managing dynamic load variations while maintaining accurate speed tracking (same results obtained in [48]).

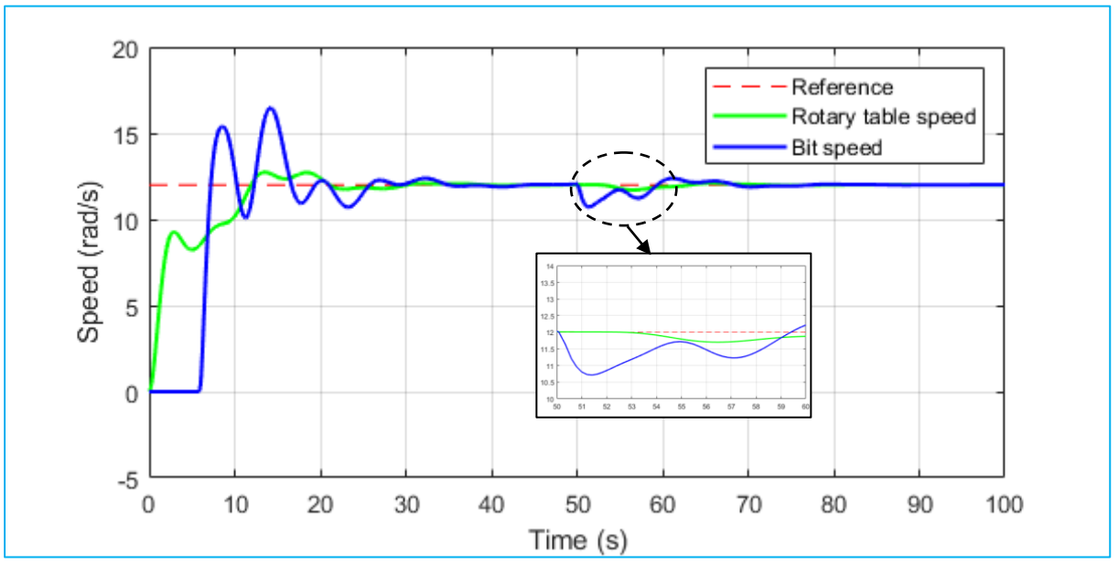

Figure III.4 Dynamic response of controlled drill string system (Reference, rotary table and bit speeds)

III.4.3 Observer Performance

This section examines the performance of the *Luenberger* observer integrated into the control loop, with the goal of evaluating its accuracy in estimating unmeasured states particularly the drill bit speed based solely on surface-level measurements.

Figure III.5 illustrates the performance of the observer designed to estimate the bit speed of the controlled drill string system. The plot compares the actual bit speed with the observed bit speed over time. Initially, the observer output rises quickly to match the real bit speed, showing a very short estimation delay during the startup transient. As the system settles, the observed bit speed closely tracks the actual speed throughout the simulation, even during oscillatory periods and steady-state operation. This close alignment indicates that the observer provides accurate and reliable estimates of the bit speed, which is critical for feedback control when direct measurement is noisy or unavailable.

The result shows the observer's high performance and suitability for real-time implementation in drill string control systems (same result obtained in [48]).

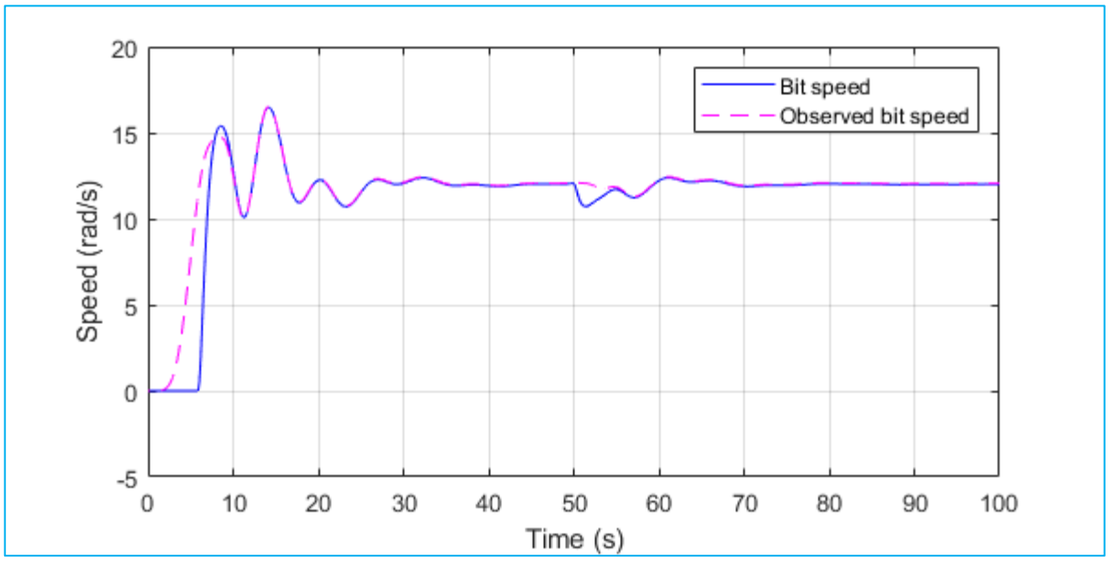

Figure III.5 *Luenberger* observer estimation of the drill string bit speed

III.5 CONCLUSION

This chapter presented a case study implementation of the 4-*DOF* drilling system torsional model and *LQR*-based control strategy developed in the second chapter. Through numerical simulations, it has been shown that the *LQR* controller augmented with integral action for speed regulation and a *Luenberger* observer for state estimation, demonstrated effective mitigation of stick-slip oscillations in closed-loop operation.

Here are the main key outcomes of this chapter:

- The open-loop analysis confirmed the system's inherent instability, with persistent stick-slip cycles under typical drilling conditions.
- The closed-loop results showed significant suppression of torsional vibrations, with improved *RPM* stability and reduced torque fluctuations.
- The observer provided accurate state estimates, enabling feasible real-world deployment.

In counterpart, here are some limitations and challenges of the investigated control strategy:

- Performance depends on model accuracy (lumped-parameter assumptions, bit-rock interaction linearization, …).
- Real-world disturbances (mud interaction, borehole friction, …) were simplified in simulations and may vary largely and randomly in practice.

To tackle these issues, one can enhance the control robustness by parameters optimization and/or adapting to prevent parametric uncertainties and external disturbances (one can use an optimal and/or adaptive *LQR* that will be the subject of the next chapter).

Chapter IV

Adaptive LQR Control via GA Optimization and ANN for Stick-Slip Mitigation

IV.1 INTRODUCTION

Stick-slip oscillations remain a critical challenge in drilling systems, leading to inefficiencies, accelerated wear, and potential equipment failure. While conventional Linear Quadratic Regulator (*LQR*) control provides a structured approach to mitigating these oscillations, its performance is highly dependent on the proper tuning of the weighting matrices (Q and R). Suboptimal tuning can lead to either insufficient damping or excessive control effort, limiting the system's adaptability under varying operating conditions.

This chapter investigates an enhanced control strategy combining Genetic Algorithm (*GA*) optimization and Artificial Neural Network (*ANN*)-based adaptation to improve the *LQR* controller's performance in suppressing stick-slip vibrations. The study is structured as follows:

First, the conventional *LQR* controller (as designed in Chapter III) is evaluated to establish a reference for stick-slip mitigation.

Then Q and R matrices are systematically tuned using a *GA* to minimize the Integral Squared Error (*ISE*) of the rotary table and/or bit speed at a given operating point, ensuring optimal transient and steady-state performance.

Finally, to enhance robustness against operating conditions variation, an *ANN* is trained to dynamically adjust *LQR* parameters based on real-time system behavior, ensuring consistent performance under different drilling scenarios.

The simulation results of the three approaches 'Conventional *LQR*, *GA*-optimized *LQR* (for a fixed operating point), and adaptive *ANN-LQR* system' will be compared to demonstrate the progressive improvements in stick-slip suppression, control efficiency, and system robustness. This chapter highlights the advantages of intelligent control tuning and adaptation, paving the way for more reliable and autonomous drilling operations.

IV.2 METHODOLOGY

To enhance the control performance of the 4-*DoF* drilling system, this study employs a hierarchical control design approach, combining the robustness of Linear Quadratic Regulator (*LQR*) theory with advanced optimization and adaptive techniques.

First, a conventional *LQR* controller with integral action is designed to ensure baseline stability and stick-slip mitigation, leveraging state feedback and optimal cost minimization (see chapter III).

Next, to address the challenge of manual tuning for the *LQR* weighting matrices (Q and R), a Genetic Algorithm (*GA*)-based optimization is applied, automating the search for parameters that minimize a cost function (*ISE* speed error of rotary table and/or bit).

Finally, to adapt to time-varying drilling conditions (such as changes in weight-on-bit or formation stiffness), an Artificial Neural Network (*ANN*)-based adaptive *LQR* is proposed, where the *ANN* dynamically adjusts the controller gains in real-time using observed system states. This hybrid methodology bridges theoretical control design with computational intelligence, aiming to improve both transient and steady-state performance under down-whole uncertainties and operating conditions variation.

IV.2.1 CONVENTIONAL *LQR* CONTROL REVIEW

As it has been explained in the second chapter, *LQR* (Linear Quadratic Regulator) is an optimal control strategy used to stabilize a dynamic system by minimizing a cost function that balances:

- ***State error*** (how far the system is from desired behavior),
- ***And control effort*** (how much energy or input is used to achieve that behavior).

The goal is to find a state feedback control law [51]:

$$u(t) = -Kx(t)$$

That minimizes the following cost function:

$$J = \frac{1}{2}\int_0^{\infty} (x(t)^T Q x(t) + u(t)^T R u(t))dt$$

Where K is the feedback gain matrix, derived to optimize system performance via solving the following Algebraic *Riccati* Equation (*ARE*):

$$A^T P + PA - PBR^{-1}B^T P + Q = 0$$

Once the matrix P is computed, the optimal gain K_x is determined as follows: $= R^{-1}B^T P$.

IV.2.2 *GA*-BASED OPTIMIZATION OF *LQR*

The performance of *LQR* control in drilling systems depends heavily on properly tuned weighting matrices Q and R. Manual tuning is inefficient and often suboptimal. To address this issue, a Genetic Algorithm (*GA*) is used to automatically optimize Q and R matrices.

The optimization objective is to minimize the Integral Squared Error (*ISE*) of the system response (the rotary table and/or bit speeds in our case) [51]:

$$ISE = \int_0^{\infty} (\alpha e_T^2(t) + \beta e_b^2(t))dt = \int_0^{\infty} \left(\alpha(\omega_d - \dot{\theta}_r)^2(t) + \beta(\omega_d - \dot{\theta}_b)^2(t)\right)dt \quad \text{(IV.1)}$$

Where α and β are weighting factors that balance rotary table and bit speed dynamic errors minimization.

This approach will improve stick-slip suppression and provide a solid foundation for more advanced adaptive control.

IV.2.2.1 GENETIC ALGORITHM PRINCIPLE

GA is an optimization algorithm that is inspired from the natural selection. It is a population-based search algorithm, which utilizes the concept of survival of fittest. The algorithm begins by randomly generating a population of candidate solutions, represented as chromosomes. Each chromosome is evaluated using a fitness function that reflects how well it solves the given problem. Two chromosomes are then selected based on their fitness values, and a single-point crossover is applied (usually) with a certain probability to generate an offspring. This offspring undergoes a uniform mutation with a specified mutation probability, producing a new solution that is added to the next generation. This cycle of selection, crossover, and mutation continues until a full new population is formed.

Genetic Algorithms are known for their strong global search capabilities, as they explore a broad solution space, dynamically adapting through crossover and mutation rates. They can also handle multiple optimal solutions simultaneously, making them well-suited for complex optimization tasks.

IV.2.2.2 CHROMOSOMES REPRESENTATION

In genetic algorithms, chromosomes represent potential solutions to an optimization problem, encoded as strings of binary digits, real numbers, or other data structures. Each chromosome consists of genes, which correspond to individual decision variables or parameters of the problem.

In our work, we used a 1×9 vector chromosome *XX* composed of 9 genes representing respectively the scaling factors of the 8 elements of the Q and one element of the R weighting matrices (see figure IV.1).

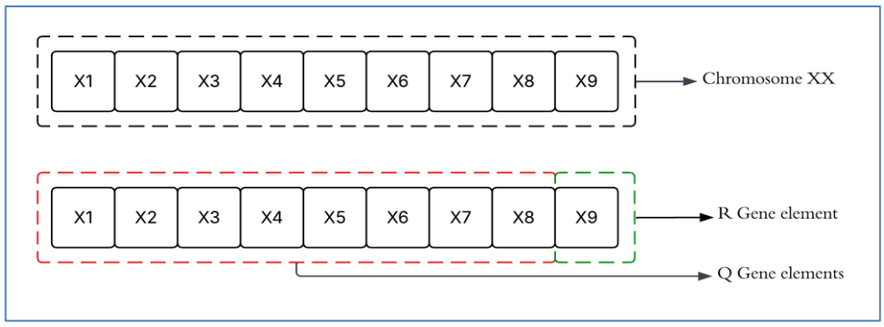

Figure IV.1 Chromosome representation of the Q & R elements scaling factors [52]

One can write then:

$$Q = \text{diag}(X_1, X_2, X_3, X_4, X_5, X_6, X_7, X_8)Q_0 \;\&\; R = X_1 R_0$$

Where: Q_0=$\text{diag}(1,1,1,10,1,1,1,1000)$ & $R_0 = 0.001$ are the weighting matrices chosen using trial and error method (see equation III.1 & III.2) [38]. So, each gene is a scaling factor for the *LQR* weighting matrices elements.

IV.2.2.3 WORKING STEPS OF THE GENETIC ALGORITHM

The algorithm begins by initializing a population of random candidate solutions (chromosomes). Each chromosome is evaluated using a fitness function to measure its quality. The fittest individuals are selected for reproduction, where crossover combines their traits to produce offspring. Mutation introduces small random changes to maintain diversity. This iterative process continues over generations, gradually improving the population until an optimal or satisfactory solution is found according to the following working steps (see also figure IV.2):

1. **Initialization**: A population of candidate solutions (chromosomes) is randomly generated.
2. **Evaluation:** Each chromosome is evaluated using a fitness function to measure its quality or performance.
3. **Selection**: Based on fitness, the best-performing individuals are selected to become parents.
4. **Crossover (Recombination):** Selected parents undergo crossover to produce offspring, combining genetic material from both.
5. **Mutation:** Offspring are slightly altered using mutation to introduce diversity.

6. **Replacement:** The new offspring replace part or all of the old population.
7. **Termination:** Steps 2–6 are repeated until a stopping condition is met (e.g., number of generations or fitness threshold).

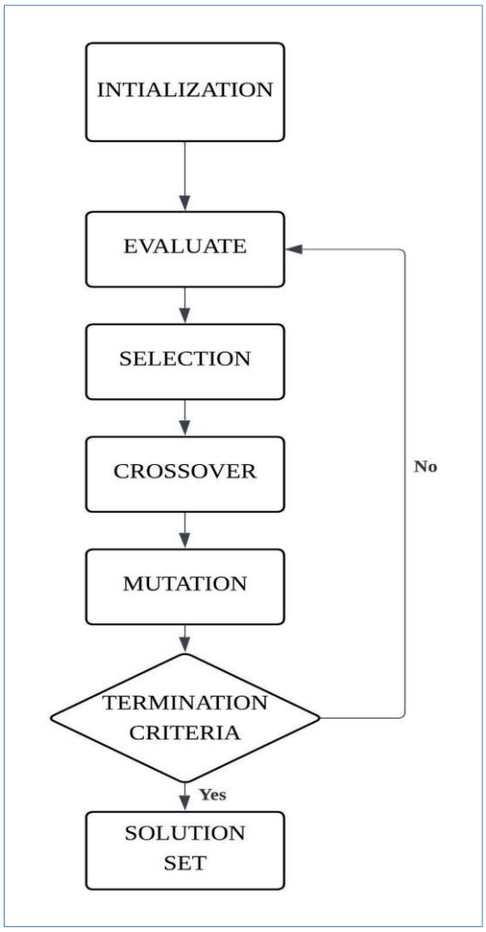

Figure IV.2 Flowchart of the working steps of *GAs* [52]

a) *Initialization*

In this phase, a population of candidate solutions is randomly generated. Each candidate, called a chromosome, encodes a potential solution to the optimization problem. Chromosomes can be represented in different ways depending on the problem domain. Common formats include binary strings, real-valued vectors, or permutations. In our case, a chromosome will encode scaling factors of the weighting matrices of the *LQ* regulator. The population size (number of individuals) significantly affects performance: a small size may lead to premature convergence, while a large size increases computational time.

b) *Evaluation*

Each chromosome is evaluated using a fitness function that quantifies how good that solution is. This function must capture the performance objectives of the problem. In our case, the fitness function is the weighted *ISEs* of rotary table and bit speeds expressed by equation (IV.1). The result is a fitness score for each chromosome, guiding the selection process.

c) *Selection*

It is an important step in genetic algorithms that determines individuals from the current population to be parents of the next generation. The goal is to prefer better solutions while maintaining genetic diversity. There are many selection techniques:

- *Roulette wheel selection:* It maps all the possible strings onto a wheel with a portion of the wheel allocated to them according to their fitness value. This wheel is then rotated randomly to select specific solutions that will participate in formation of the next generation
- *Tournament Selection:* The individuals are selected according to their fitness values from a stochastic roulette wheel in pairs. After selection, the individuals with higher fitness value are added to the pool of next generation
- *Elitism:* The best individuals are automatically passed to the next generation without alteration.

d) *Crossover*

It is a genetic operator that creates new offsprings (solutions) by combining the genes of two parent chromosomes. It mimics biological recombination and enables the exchange of good traits between individuals. There are two main crossover techniques:

- *Single-Point Crossover*: A point is chosen, and segments are swapped, see the following figure.

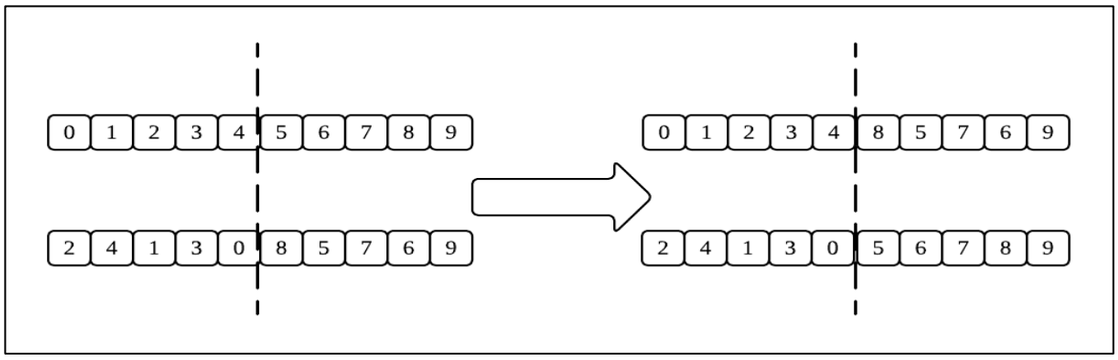

Figure IV.3 Swapping genetic information after a single-point crossover process [52]

- *Two-Point Crossover:* Two points are chosen, and the middle segments are exchanged, see the following figure.

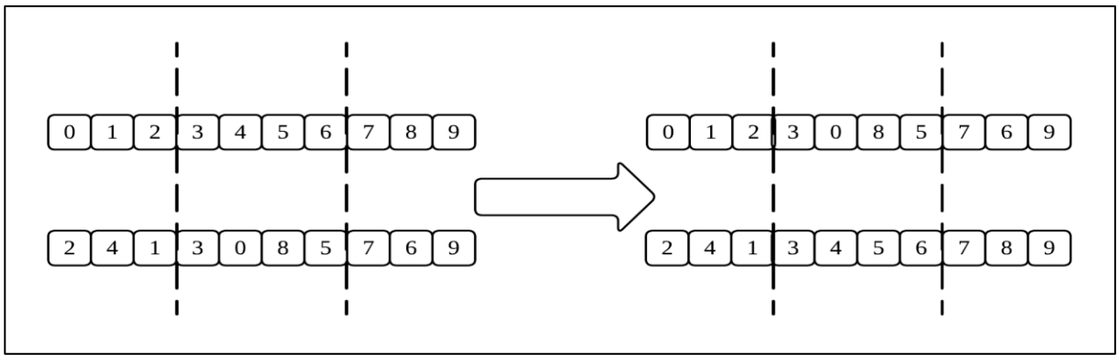

Figure IV.4 Swapping genetic information after a two-point crossover process [52]

d) *Mutation*

Mutation introduces random changes to individual genes in a chromosome. It is an operator that maintains the genetic diversity from one population to the next population. This prevents the algorithm from getting trapped in local optima and encourages exploration of the solution space. Mutation occurs after crossover and affects offspring by altering one or more of their genes. There are three main techniques of the mutation:

- *Displacement mutation:* In displacement mutation, a substring (a sequence of genes) is selected and removed from its original position, then inserted into a different random position in the chromosome. In the example of figure IV.5, we:
  1- Select a segment ([3, 4, 5] in this example)
  2- Remove segment (we obtain the string [0, 1, 2, 6, 7, 8, 9])
  3- Insert after 1(we obtain the mutated chromosome [0, 1, 3, 4, 5, 2, 6, 7, 8, 9]).

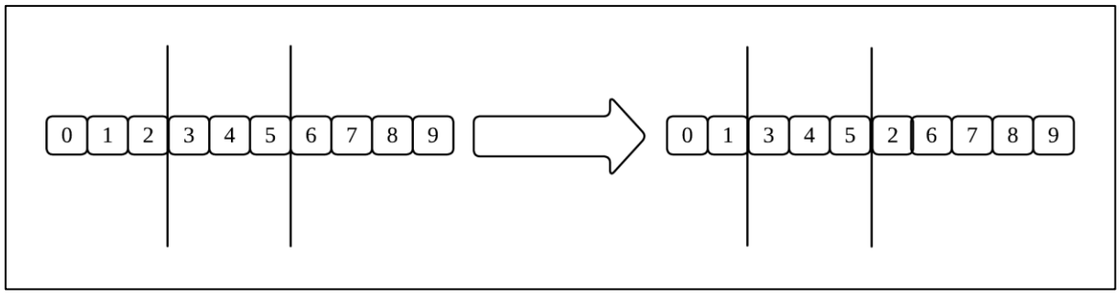

Figure IV.5 Example of a displacement mutation [52]

- *Simple inversion mutation :* In this case, a segment of the chromosome is selected, and the order of genes within that segment is reversed (inverted). In the example of figure IV.6, we:
  1- Select a segment (for example [4, 5, 6, 7])
  2- Resverse the segement elements or genes (we obtain the mutated chromosome [0, 1, 2, 3, 7, 6, 5, 4, 8, 9]).

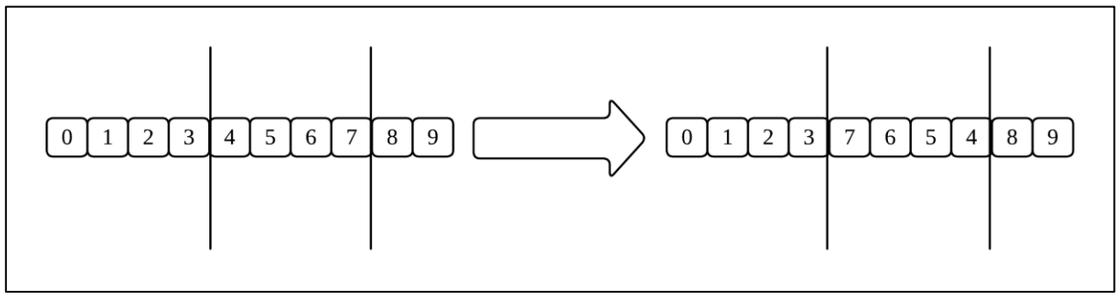

Figure IV.6 A simple inversion mutation [52]

- *Scramble mutation:* A section of the chromosome is selected randomly, and the genes within this section are randomly scrambled. For example (see figure IV.7):
  1. Select randomly a segment (for example [2, 3, 4, 5])
  2. Scramble its genes by order randomizing (we obtain foe example the following mutated chromosome [0, 1, 5, 3, 4, 2, 6, 7, 8, 9]).

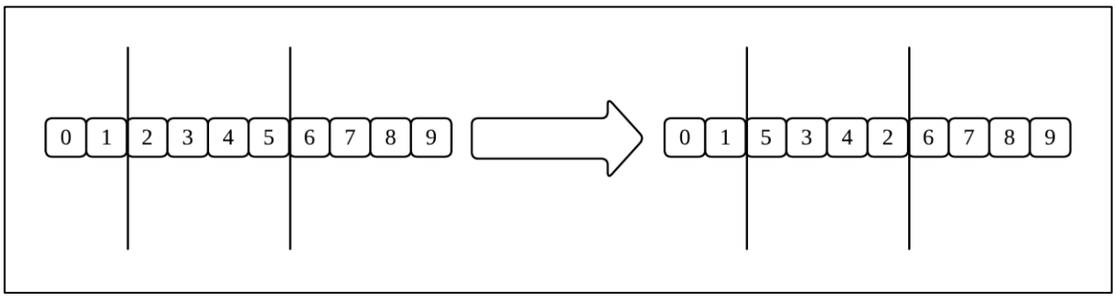

Figure IV.7 A scramble mutation [52]

e) *Termination*

The algorithm continues evolving the population through evaluation, selection, crossover, mutation, and replacement until a stopping condition is met. This could be:

- a fixed number of generations,
- a target fitness level,
- or a lack of improvement over several iterations (stall generations).

Once the condition is met, the best solution found is reported.

IV.2.3 *ANN*-BASED ADAPTIVE *LQR*

This section presents the design and implementation of an Artificial Neural Network (*ANN*)-based adaptive control system to enhance the performance of the *LQR* controller under time-varying of the drilling system operating conditions.

IV.2.3.1 *ANN* architecture

The used *ANN* is structured as a feed-forward neural network, typically a multi-layer perceptron (*MLP*) topology (see figure IV.8).

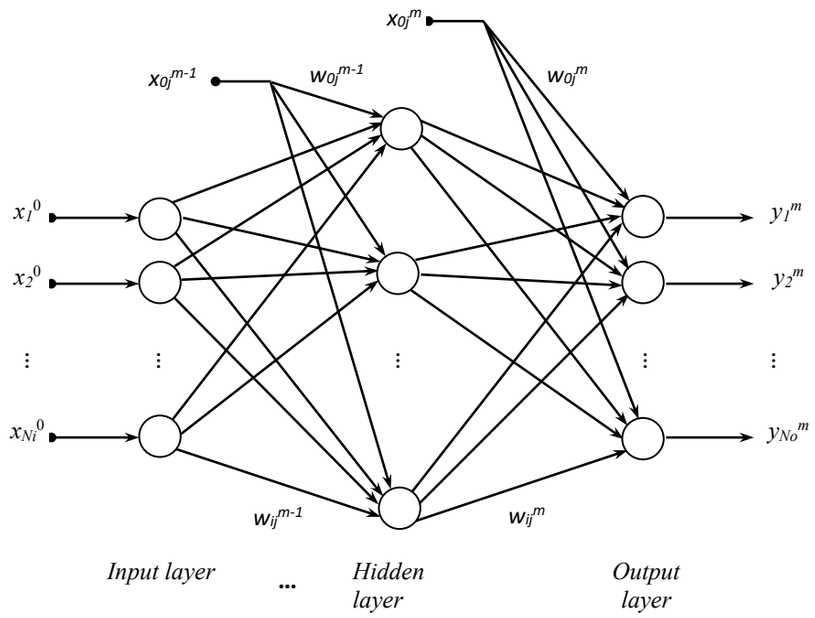

Figure IV.8 A multilayer perceptron [53]

Where x_i^0 is the i^{th} input, N_i is the inputs number; y_j^0 is the j^{th} output, N_o is the outputs number; w_{ij}^m is the synaptic weight connecting the j^{th} neuron of the m^{th} layer to the i^{th} neuron of the previous layer.

This *MLP* maps the current drilling system operating conditions to optimal or near-optimal adjustment of the *LQR* weighting matrices. It has the following characteristics:

- The inputs (N_i=2 in our case) of this *ANN* are the key operating parameters of the drilling system (desired rotary speed $x_1^0 = \omega_d$ (*RPM*) and the Weight-on-Bit (x_2^0=*WoB*)).
- The outputs (N_o=9 in our case) of the neural network are the scaling factors of the diagonal elements of *Q* and *R* ($XX_{1\ to\ 9}$) used to tune the baseline *LQR* configuration.
- The *ANN* is composed of four hidden layers of 20, 30, 50 and 70 neurons respectively, providing a balance between model complexity and generalization ability.
- The activation functions that are used for the hidden layers are *tanh* (Hyperbolic tangent) to introduce non-linearity, enabling the *ANN* to learn complex patterns; while *ReLU* (Rectified Linear Unit defined by: $y(X)=\max(0,X)$) is used for the output layer.

IV.2.3.2 Training Algorithm

The *Levenberg-Marquardt* back-propagation algorithm is selected due to its fast convergence and high accuracy for function approximation tasks. It allows us to tune the synaptic weights of the *ANN* as follows [54]:

$$w_{ij}^m(n+1) = w_{ij}^m(n) - \left[H(n) + \mu_u \mathbf{I}\right]^{-1} g(n) \quad \text{(IV.2)}$$

Where w_{ij}^m is the synaptic weight connecting the j^{th} neuron of the m^{th} layer to the i^{th} neuron of the previous layer; *n* is the iteration number, **I** the identity matrix, *H* and *g* are the approximated *Hessian* matrix and gradient respectively.

The training process is performed according to the following steps (see figure IV.9):

- ***Dataset generation:*** A representative dataset is generated by running *GA*-optimized *LQR* simulations across a wide range of drilling conditions, capturing the corresponding optimal *Q* and *R* values. We have varied ω_d from *8* to *20* with a step of *2* rad/s and the *WoB* from 50 kN to 150 kN with a step of *5 kN* to build suitable optimized database to train the *ANN* of N_s=147 samples of couples inputs/outputs data.
- ***Offline training:*** The *ANN* is trained using this dataset in an offline environment. The objective is to minimize the Mean Squared Error (*MSE*) between the predicted and targeted *Q*/*R* values [55]:

$$MSE = \frac{1}{2}\sum_1^{Ns} \varepsilon^T \varepsilon = \frac{1}{2}\sum_1^{Ns} (XX_d - XX)^T (XX_d - XX) \quad \text{(IV.2)}$$

- ***Validation:*** The dataset is split into training, validation, and test sets. Performance is evaluated through the calculation of the *MSE*.

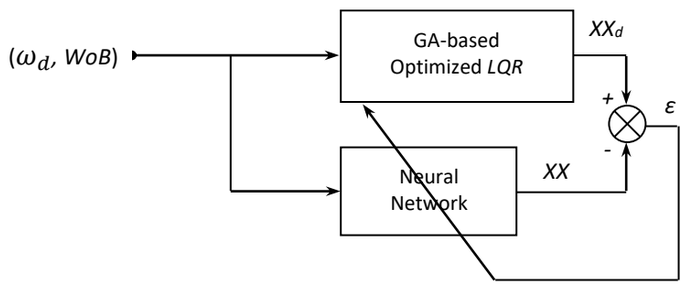

Figure IV.9 *ANN* training process [53]

IV.2.3.3 Real-time adaptation

Once trained, the *ANN* is deployed as an online adaptation module. During operation, it continuously receives real-time data (ω_d or *RPM*, *WoB*) and updates the *LQR* controller parameters accordingly. This enables the control system to maintain optimal performance despite changes in drilling dynamics and operating conditions. The *ANN*'s low computational time ensures compatibility with real-time execution environments.

IV.3 Simulation Results and Analysis

To validate the effectiveness of the investigated *LQR*-based control strategies (conventional, *GA*-optimized, and *ANN*-adaptive), this section presents a comparative analysis of simulation results under realistic drilling conditions. The evaluation focuses on three key aspects:

- Closed-loop basic *LQR* performance to demonstrate baseline improvements in terms of stick-slip oscillations mitigation.
- Comparison between control strategies (*LQR*, *GA-LQR*, *ANN-LQR*) in terms of transient response, steady-state error, and robustness to disturbances.

The simulated transient of the closed loop drilling system is the same of that of chapter III. In fact, the reference speed (ω_d=12 *rpm*) represents the desired setpoint that the *LQR* controller aims to track. Initially, both the rotary table and the drill bit are at standstill. During this initial phase $t\epsilon$[0 50]s, the *WoB* is maintained at 97.347 kN. For $t\epsilon$[50 100]s, the *WoB* is increased to 110 kN.

IV.3.1 Conventional *LQR*

The controller exhibits acceptable transient and steady state performance under these disturbance conditions, but its fixed parameters result in suboptimal transient response and higher overshoots especially in the bit speed transient under varied drilling conditions. The controller struggles (more to less) to fully suppress stick-slip oscillations when faced with changes in weight-on-bit or speed (see figure IV.10)

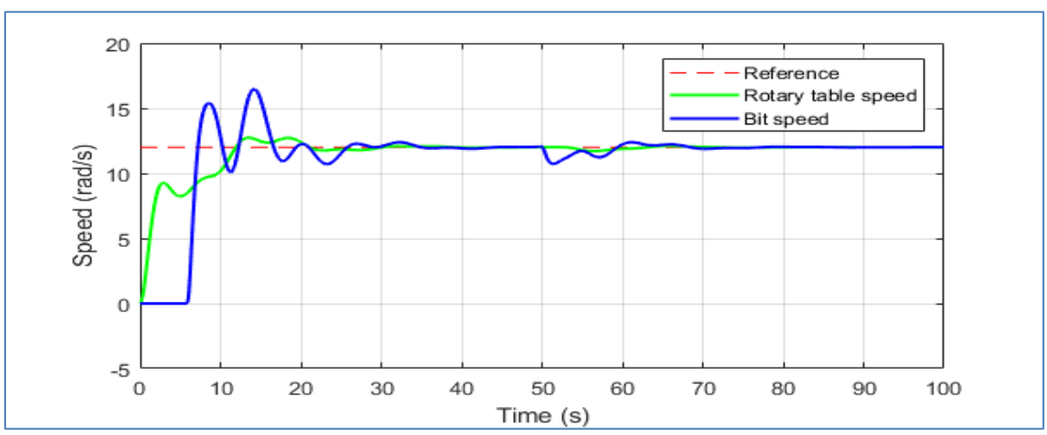

Figure IV.10 Dynamic response of the drill string system controlled by a basic *LQR*

In this case, a comparison between open-loop (see figure III.2) and closed-loop performance clearly demonstrates the benefit of the feedback basic *LQR* control in mitigating stick-slip vibrations. In open-loop operation, significant oscillations occur due to nonlinear bit-rock interactions, leading to unstable bit speed and rotary table fluctuations. Under closed-loop control, the designed *LQR*-based controller effectively suppress these oscillations, improving speed tracking and stabilizing the drilling process even under varied load conditions.

IV.3.2 *GA*-OPTIMIZED *LQR*

The Genetic Algorithm (*GA*)-optimized *LQR* was performed using an aggregated multi-objective cost function that considers both bit speed and rotary table speed errors, weighted by the coefficients α and β (see equation IV.1).

For this purpose, we have used the Genetic Algorithm Tool (*gatool*) that provides a graphical interface for configuring and running genetic algorithm (*GA*) optimizations under *MATLAB* environment. Here are the main steps to set up and use '*gatool*', see figure IV.11:

- ***Launch the tool:*** Open *MATLAB* and type *gatool* in the command window, or navigate to the Optimization Tool (*optimtool*) and select (*ga*) from the solver dropdown menu.
- ***Define the problem by:***
  - ✓ Entering the function file name (@drillstring_fit in our case) that calculates the cost function of equation IV.1 to be minimized.
  - ✓ Giving the number of variables by specifying the dimensions of the problem (9 in our case).
  - ✓ Adding linear/nonlinear constraints, bounds, or integer constraints if applicable. In our case, we have only added lower and upper bounds that delimits the search space (The 9 scaling factors to tune vary in [0.01 100]).
- ***Configure algorithm main settings by:***
  - ✓ Setting a population type (default: *Double Vector*) and size (default: 20).
  - ✓ Choosing methods of selection, crossover (and its fraction) and mutation (and its rate), for example *Roulette*, *single point* (0.8), *uniform* (0.01).
  - ✓ Define stopping criteria: *Generations* (100 in our case), *Stall generations* (50 in our case), …
  - ✓ Choose functions to be plotted (*Best fitness & best individual*, …).
- ***Run the Optimization by:***
  - ✓ Clicking on '*Start*' to execute the *GA*. Monitor progress in the *Status and Results* panel.
  - ✓ Export results from the final solution.

Three distinct optimization scenarios were evaluated:

- ***Case 1* ($\alpha = 1$ & $\beta = 0$):** The optimization focused solely on minimizing the bit speed error. As a result, the controller provided excellent suppression of bit stick-slip vibrations with minimal tracking error on the bit speed. However, the rotary table speed exhibited slightly higher fluctuations due to the lack of weighting on its performance during optimization (see Figure IV.12.a).
- ***Case 2* ($\alpha = 0$ & $\beta = 1$):** Here, the optimization emphasized rotary table speed regulation at the expense of bit speed tracking. While the rotary table speed followed its reference closely with minimal oscillations, stick-slip behavior at the bit became more pronounced, resulting in higher bit speed fluctuations (see figure IV.12.b).

- ***Case 3* ($\alpha = 1$ & $\beta = 1$):** This configuration equally balanced bit speed and rotary table speed tracking. The resulting controller demonstrated a good trade-off between suppressing stick-slip vibrations and maintaining stable rotary table dynamics. Both bit and rotary table speeds closely followed their references with reduced oscillations, and the control effort remained within acceptable limits (see figure IV.12.c).

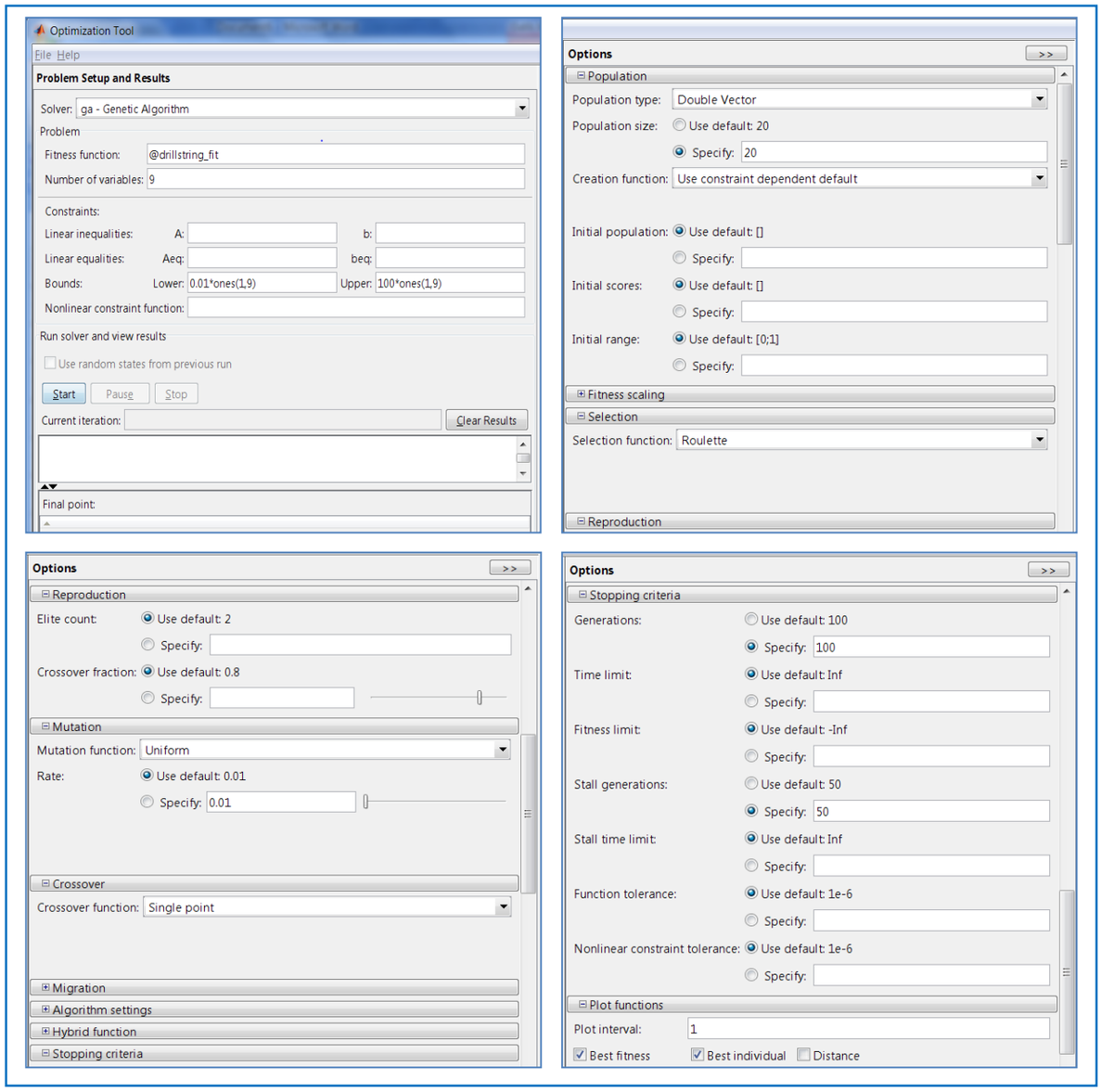

Figure IV.11 *MATLAB* graphical interface '*gatool*' configuration & main settings

The following table summarizes the results obtained for different weighting factors cases:

Table IV.1 Cost function for different weighting factors cases

		GA-based *LQR* with different weighting factors of the cost function		
	Basic LQR	$\alpha = 1 \,\&\, \beta = 0$	$\alpha = 0 \,\&\, \beta = 1$	$\alpha = 1 \,\&\, \beta = 1$
$\boldsymbol{ISE1 \times 10^{-2}}$	9.8664	9.7163	14.4848	9.8126
$\boldsymbol{ISE2 \times 10^{-2}}$	2.1821	1.9896	0.3568	2.1290

Where *ISE1* and *ISE2* are the integral squared errors of the bit and rotary table speeds respectively.

These results clearly show the influence of the cost function weighting factors on the control performance. Note that '***Case 1* ($\alpha = 1$ & $\beta = 0$)**' focused on minimizing bit speed error and achieved the best stick-slip oscillations suppression on the bit speed; while '***Case 2* ($\alpha = 0$ & $\beta = 1$)**' emphasized rotary table performance, strongly reducing *ISE2*, but with significant degradation in bit speed regulation.

On the other hand, *'**Case 3* ($\alpha = 1$ & $\beta = 1$)**' provided a balanced trade-off, improving both bit and rotary table speed errors compared to the conventional *LQR* and the two previous cases. This confirms that *GA*-based tuning offers flexible adjustment depending on specific control priorities.

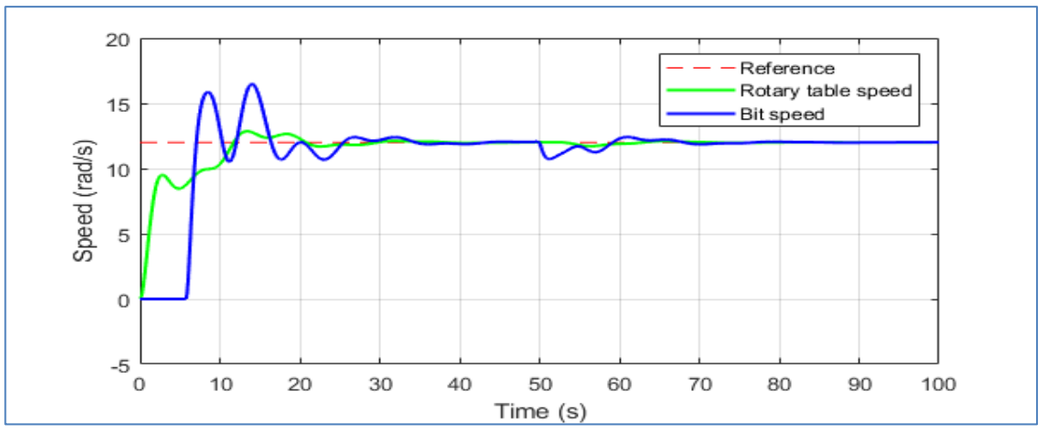

a) Case of ($\alpha = 1$; $\beta = 0$)

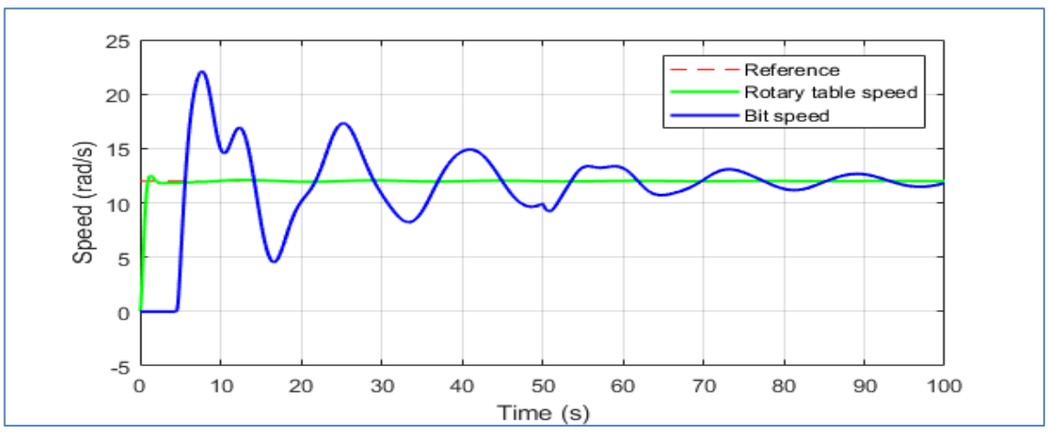

b) Case of ($\alpha = 0$; $\beta = 1$)

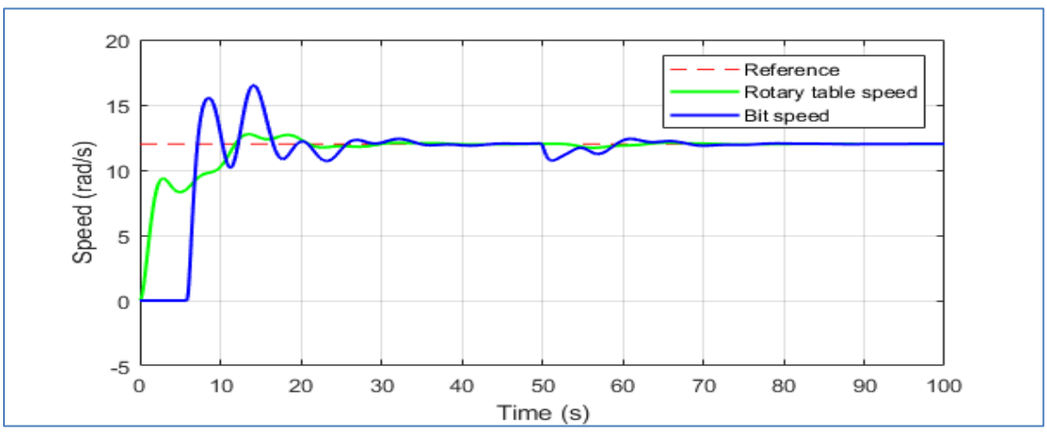

c) Case of ($\alpha = 1$; $\beta = 1$)

Figure IV.12 Dynamic response of the drill string system controlled by *GA-based LQR*

Now, to evaluate the robustness of the controller under more severe drilling conditions, the Weight-on-Bit (*WoB*) was further increased by 25% (from 97.347 kN to 1.25×97.347 kN at t=0s and from 110 kN to 1.25×110 kN at t=50 s), while the desired rotational speed (ω_d) is augmented by 33% from 12 rad/s to 16 rad/s.

In this case, oscillations occur due to nonlinear bit-rock interactions, leading to transient oscillated bit and fluctuated rotary table speeds in the case of the basic *LQR* controller (figure IV.13.a) comparatively to the initially *GA*-optimized based *LQR* controller with fixed *Q* & *R* (figure IV.13.b). As expected, the *GA*-optimized based *LQR* controller with retuned *Q* & *R,* suppress more these oscillations, improving speed tracking and stabilizing the drilling process even under these severe varied load and *RPM* conditions (figure IV.13.c).

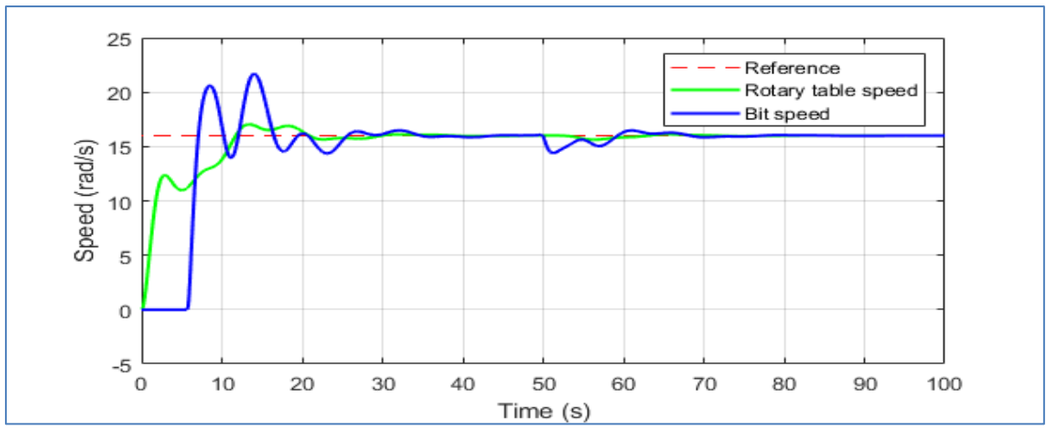

a) Case of basic *LQR* controller

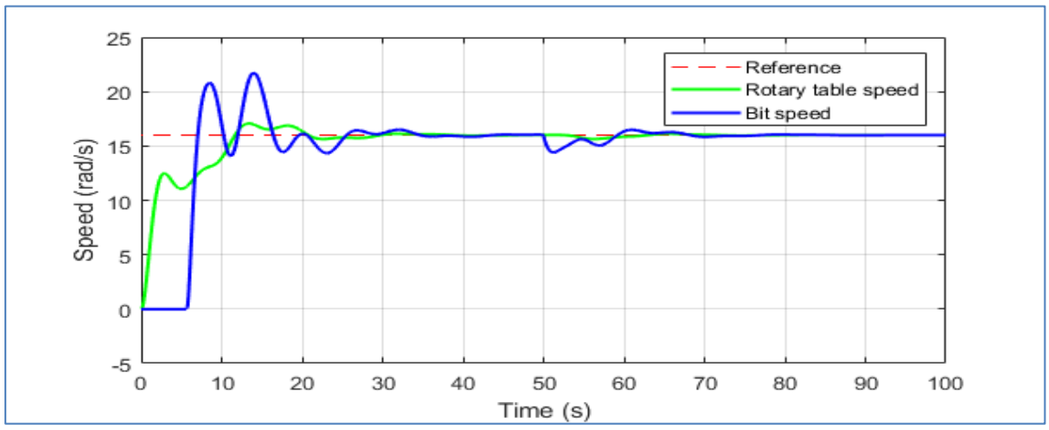

b) Case of initially *GA*-optimized based *LQR* controller with fixed *Q* & *R*

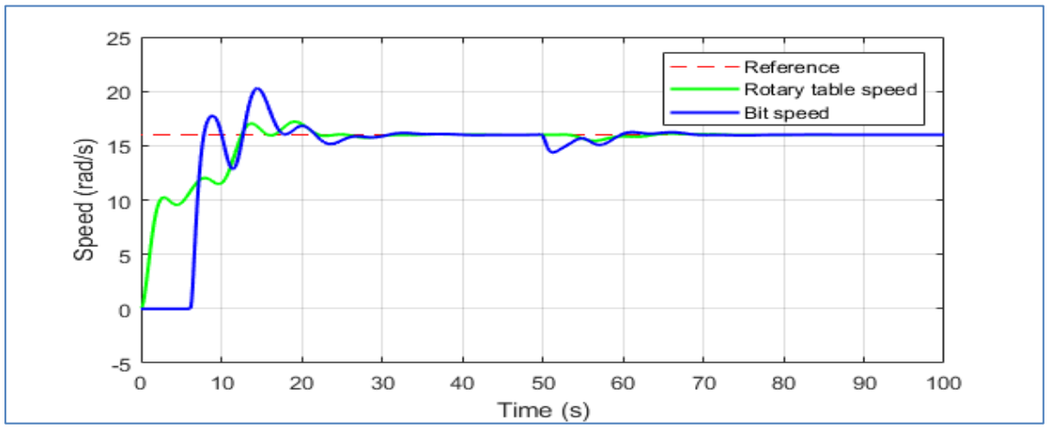

c) Case of *GA*-optimized based *LQR* controller with retuned *Q* & *R*

Figure IV.13 Dynamic response of the drill string system controlled by different *LQR-based techniques*

Moreover, the table below presents the resulting performance for different Q and R configurations in the case of ($\alpha = 1$, $\beta = 1$) under these updated conditions.

Table IV.2 *Different LQR* controller's robustness against operating conditions variation

		Weighting factors of the cost function ($\alpha = 1$ & $\beta = 1$)	
	Basic LQR	Initially *GA*-optimized and fixed Q & R	*GA*-retuned Q & R
$ISE1 \times 10^{-2}$	25.7752	25.8356	25.0791
$ISE2 \times 10^{-2}$	15.7967	15.7947	15.8115

The results of these tests clearly demonstrate that every time the drilling parameters, such as weight-on-bit (*WoB*) and/or table reference speed (ω_d), change significantly, the optimal Q and R matrices must be re-tuned to maintain satisfactory control performance. Although the basic *LQR* design exhibits some robustness under varying operating conditions, re-optimization remains necessary to achieve the best compromise between bit speed regulation and rotary table stability. This repeated tuning requirement highlights a major limitation of fixed-parameter controllers (even optimized) and emphasizes the need for an adaptive approach. By introducing an Artificial Neural Network (*ANN*), the control system can automatically adjust Q and R in real-time, eliminating manual re-tuning and maintaining consistent control performance as drilling conditions evolve.

IV.3.3 *ANN*-BASED ADAPTIVE *LQR*

The Artificial Neural Network (*ANN*)-based adaptive *LQR* was performed using a trained feedforward *ANN* trained through the minimization of the *MSE* of equation (IV.2).

First, let us show briefly how to set up the '*nntool*' of *MATLAB* that we have used to create a feedforward *ANN* for fitting Q & R elements corresponding to the different operating conditions of (ω_d & *WoB*). The '*MATLAB Neural Network Toolbox*' provides '*nntool*' (Neural Network Tool) for designing and training feedforward *ANNs*. The following steps describe briefly how to configure a network for fitting purposes, see figure IV.14:

- ***Launch 'nntool':*** Open *MATLAB* and type '*nntool*' in the *Command Window*.
- ***Import data:*** Load inputs (In our case *Xnn* is a double rows matrix with N_s =147 column elements as couples of (ω_d & *WoB*)) and targets (In our case *XX* is a matrix of *9* rows and N_s =147 column elements of the 9 scaling factors of Q & R matrices) datasets as *MATLAB* variables. In *nntool*, click '*Import*' to assign *Xnn* as *Inputs* and *XX* as *Targets*.
- ***Network architecture creation and settings:*** In *nntool*, click '*New*' to define the *ANN* architecture that is named automatically '*network1*'. Then select *Xnn* as *Inputs* and *XX* as *Targets*. Specify the *ANN* type (Feed-forward with back propagation training in our case), the number of hidden layers and neurons (4 hidden layers of 20, 30, 50 and 70 neurons respectively), activation functions (*tansig* in our case), training algorithm ('*trainlm*': *Levenberg-Marquardt* algorithm which is convenient for small/medium datasets) and set the performance metric or the training function (*MSE*: *MSE* of equation IV.2 in our case).

- ***Viewing, training and evaluating the created ANN:*** In *nntool*, select '*network1*' and open it. Then one can view its architecture, train it, simulate or evaluate it after the training operation. Click '*Train*' to start training. Monitor progress using the validation check stopping criterion. After training, evaluate performance using '*Simulate*' and the test dataset.
- ***Export results:*** Export the trained network results (*network1*, *network1_outputs*, *network1_errors*) to the workspace for checking and predictions using *sim*(*network1*, *newXnn*). At this level, the *ANN* (*network1*) is ready to be used to estimate the 9 scaling factors of the *Q* & *R* weighting matrices of the *LQR* adaptive controller.

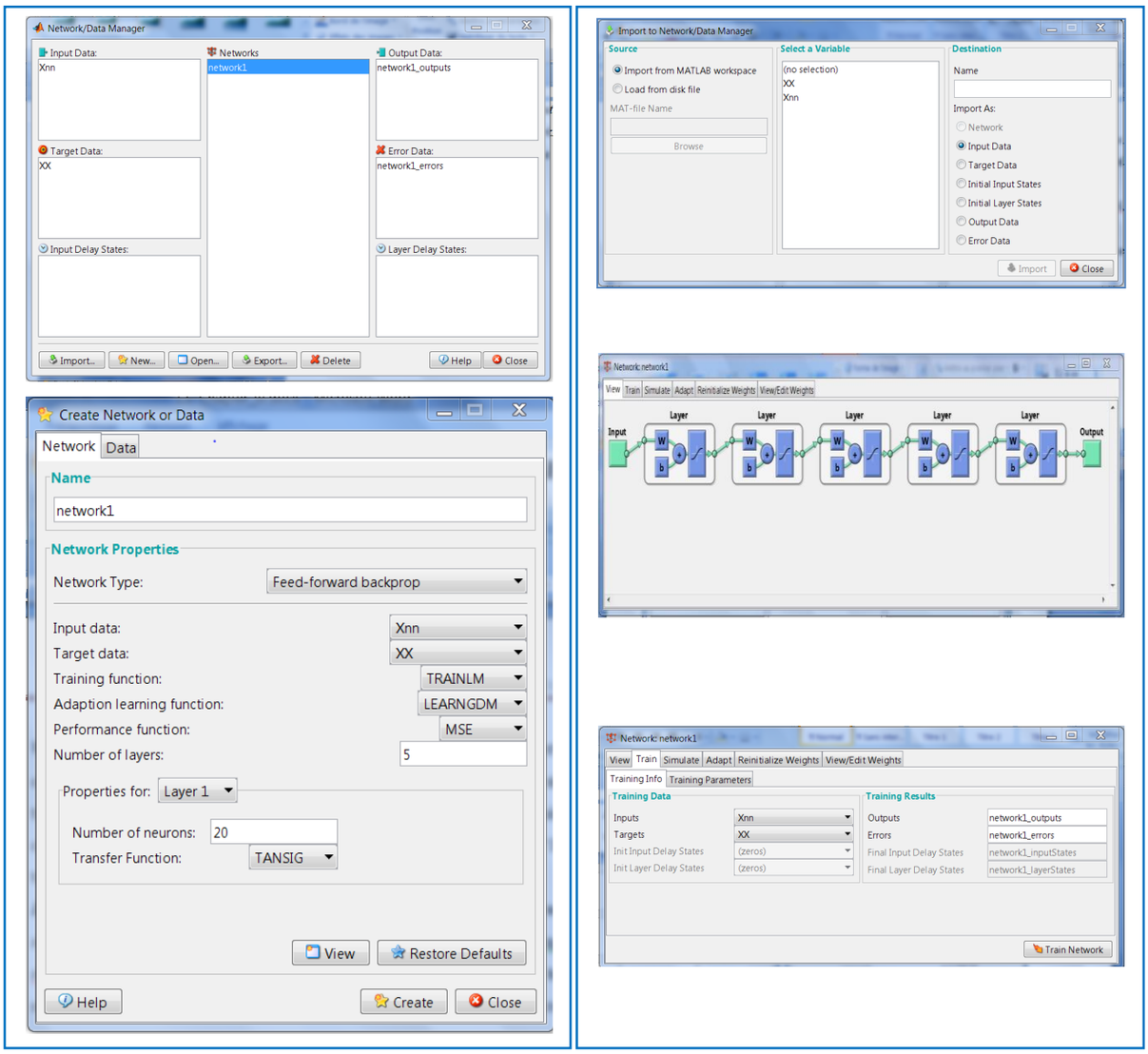

Figure IV.14 *MATLAB* graphical interface '*nntool*' configuration & main settings

After training, the *ANN* outputs track accurately their targets with an absolute error less than 1%. For example, the figure IV.15 shows the different targets and *ANN* outputs corresponding to the variables XX_1 & XX_9 which are the scaling factors of the element Q_{11} of the *Q* weighting matrix and the *R* weighting matrix (respectively) of the basic *LQR* controller.

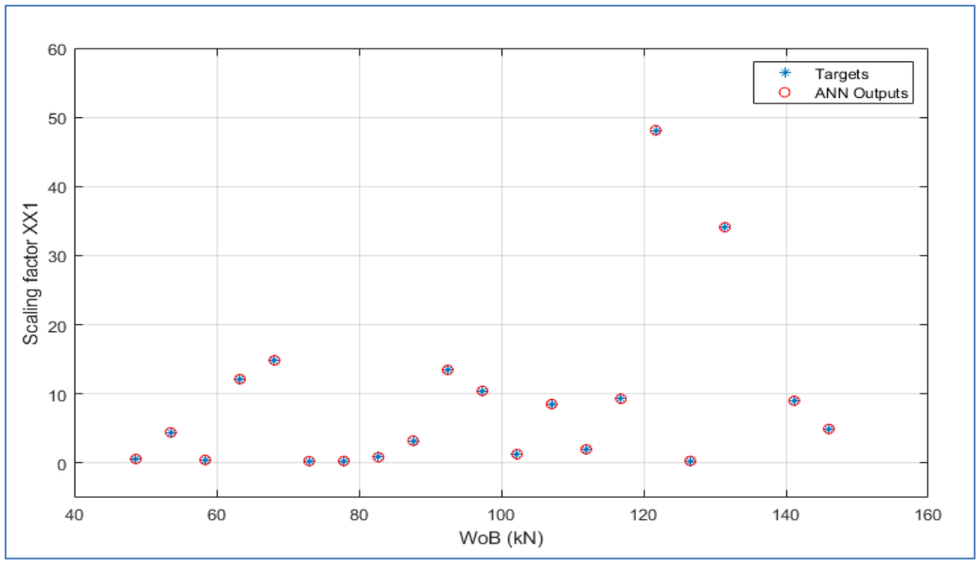

a) Case of the *XX1* scaling factor

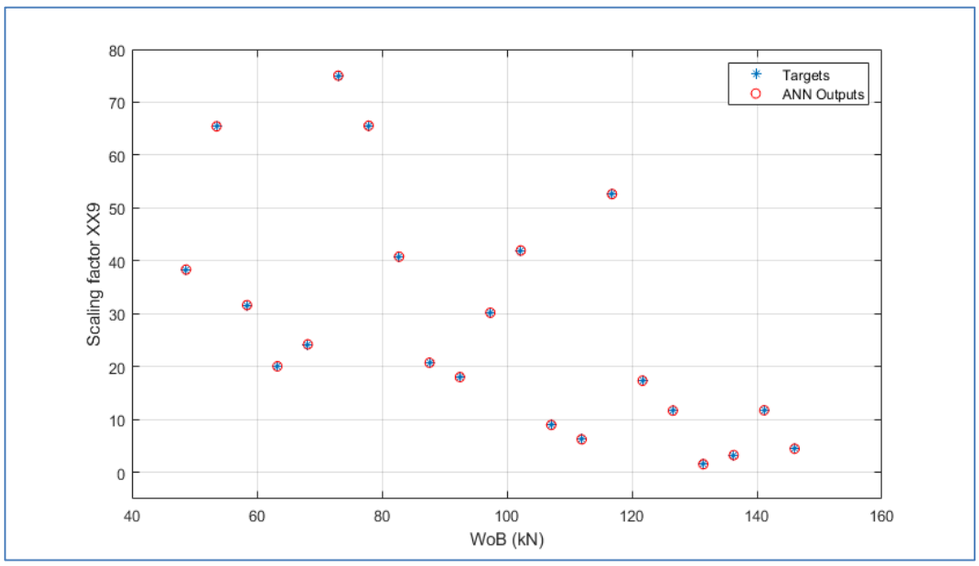

b) Case of the *XX9* scaling factor

Figure IV.16 Some *ANN* outputs and their targets

IV.3.4 Comparative Performance of Different *LQR*-based Controllers

Briefly, the effectiveness of the adaptive *LQR*-based *GA-ANN* controller in suppressing stick-slip vibrations surpasses that of the *GA*-based *LQR* and the traditional *LQR* approach.

While the basic *LQR* offers stability, its fixed gain structure limits adaptability to varying operating conditions, often resulting in suboptimal performance when system dynamics change. The *GA*-based *LQR* enhances control efficiency by optimizing gain parameters, reducing overshoot and improving transient response, but it remains static after optimization, lacking real-time adaptation. In contrast, the adaptive *LQR*-based *GA-ANN* controller integrates intelligent learning mechanisms that dynamically adjust gains based on the trained *ANN* model, leading to superior vibration suppression, reduced energy consumption, and enhanced robustness in uncertain environments.

Simulation results reveal that the adaptive approach leads to a better cost function minimization (implicitly characterized by faster settling time and lower steady-state error), demonstrating its superiority in maintaining system stability under fluctuating conditions, see table IV.3.

Table IV.3 *Different LQR* controller's cost function comparison for some testing set points

		Weighting factors of the cost function ($\alpha = 1$ & $\beta = 1$)	
	Basic LQR	Initially *GA*-optimized and fixed *Q* & *R*	*GA*-retuned *Q* & *R*
WoB=97347×0.5 kN & ω_d=8 rad/s			
$\boldsymbol{ISE1\times10^{-2}}$	23.2821	24.3345	23.1568
$\boldsymbol{ISE2\times10^{-2}}$	18.8781	20.2236	18.6941
WoB=97347×1.5 kN & ω_d=8 rad/s			
$\boldsymbol{ISE1\times10^{-2}}$	32.4811	34.7928	27.6362
$\boldsymbol{ISE2\times10^{-2}}$	20.2352	22.7230	16.3259
WoB=97347×0.5 kN & ω_d=13 rad/s			
$\boldsymbol{ISE1\times10^{-2}}$	9.6177	9.4499	9.5558
$\boldsymbol{ISE2\times10^{-2}}$	2.7869	3.6576	2.7188
WoB=97347×1.25 kN & ω_d=13 rad/s			
$\boldsymbol{ISE1\times10^{-2}}$	11.5950	12.4330	11.5640
$\boldsymbol{ISE2\times10^{-2}}$	2.7221	3.8136	2.1335
WoB=97347×1.5 kN & ω_d=13 rad/s			
$\boldsymbol{ISE1\times10^{-2}}$	12.6544	13.9152	12.1883
$\boldsymbol{ISE2\times10^{-2}}$	2.7459	3.9855	1.8190
WoB=97347×0.5 kN & ω_d=18 rad/s			
$\boldsymbol{ISE1\times10^{-2}}$	46.0180	43.4831	42.8757
$\boldsymbol{ISE2\times10^{-2}}$	35.1140	34.9310	34.8808
WoB=97347×1.5 kN & ω_d=18 rad/s			
$\boldsymbol{ISE1\times10^{-2}}$	45.2698	43.9393	43.5476
$\boldsymbol{ISE2\times10^{-2}}$	33.9294	33.3942	33.2506

In fact, *ISE1*% (*ISE*2%) has been reduced by more than 14% (30%) and 20% (50%) respectively in some cases of retuned-*LQR* compared to basic and *GA*-based *LQRs* respectively.

IV.4 CONCLUSION

This chapter presented an advanced control strategy for mitigating stick-slip oscillations of a 4-*DoF* drilling system by integrating Genetic Algorithm (*GA*) optimization and Artificial Neural Network (*ANN*)-based adaptation of a conventional *LQR* controller. The study demonstrated a progressive improvement in control performance through three key stages:

- Conventional *LQR* control served as the baseline, confirming that while effective, its performance is highly sensitive to the manual tuning of *Q* and *R* matrices, leading to suboptimal damping under varying conditions.
- *GA*-Optimized *LQR* by minimizing the Integral Squared Error (*ISE*) of rotary table and/or bit speeds, allowed an automated tuning significantly enhanced transient response and steady-state accuracy for a given operating point, outperforming the manually tuned *LQR*.
- *ANN*-Adaptive *LQR* has been used successfully to ensure robustness across different operating conditions. In fact an *ANN* was trained to dynamically adjust *LQR* parameters in real time, maintaining optimal performance even as drilling dynamics evolved for different operating conditions.

General Conclusion

General Conclusion

This dissertation has addressed the critical challenge of Stick-Slip Oscillation (*SSO*) mitigation in drilling systems through advanced modeling, control, and optimization techniques. The study focused on elaborating a 4-*DOF* torsional drilling model, designing an *LQR* controller with integral action, and enhancing its performance using Genetic Algorithm (*GA*) optimization and Artificial Neural Network (*ANN*)-based adaptation.

This research makes significant footsteps in addressing *SSO* issue by integrating advanced control theory with computational intelligence. The study begins by establishing a high-fidelity 4-*DoF* drilling model, which accurately captures torsional dynamics and serves as the foundation for controller development. It is based on the *LQR* controller with integral action, which effectively stabilizes rotary speed while compensating for steady-state errors – a notable improvement over conventional methods. Further enhancement is achieved through Genetic Algorithm (*GA*) optimization, where the automated tuning of Q and R weighting matrices minimizes the Integral Squared Error (*ISE*) of both rotary table and bit speeds, ensuring optimal performance across varied operating conditions. The most adaptive solution emerges from the Artificial Neural Network (*ANN*)-based controller, which dynamically adjusts *LQR* parameters in real time, demonstrating superior robustness compared to static and *GA*-optimized *LQR* variants. Through comprehensive simulations, the study systematically validates each approach, with comparative results highlighting the progressive improvements in *SSO* suppression from baseline *LQR* to intelligently optimized and adaptive control architectures.

The findings of this dissertation provide a substantial key-feature for the oil and gas industry, offering practical solutions to enhance drilling efficiency and equipment longevity. By transitioning from heuristic tuning to model-based and *AI*-driven control, the adopted methods reduce reliance on trial-and-error adjustments, lowering operational costs and save time.

The *ANN*-adaptive framework, in particular, paves the way for self-regulating drilling systems capable of responding to unpredictable down-hole conditions.

As a perspective, future work should focus on real-world validation through field trials or scaled rig experiments, bridging the gap between simulation and industrial deployment.

Additionally, exploring deep reinforcement learning could further refine adaptability, while extending the model to incorporate coupled axial-torsional-lateral vibrations would address more complex drilling dynamics.

In conclusion, this study successfully bridges control theory, evolutionary optimization, and machine learning to enhance drilling efficiency, paving the way for smarter, more resilient drilling automation systems.

Bibliography

Bibliography

[1] J.D. Jansen, '*Nonlinear rotor dynamics as applied to oilwell drillstrings*', Journal of Sound and Vibration, Vol. 147, No. 1, pp. 115–135, 1991.

[2] R.W. Tucker and C. Wang, '*An integrated model for drill-string dynamics*', Journal of Sound and Vibration, Vol. 224, No. 1, pp. 123–165, 1999.

[3] A. Kyllingstad and H. Førre, '*Simulation of stick-slip in drilling systems*', SPE Drilling & Completion, Vol. 13, No. 1, pp. 35–39, 1998.

[4] L. Gao and W.A. Gray, '*Adaptive control of stick-slip vibrations in oilwell drillstrings*', Control Engineering Practice, Vol. 11, No. 5, pp. 531–542, 2003.

[5] Y. Liu, Y. Zhang, H. Liu and M. Liu, '*Control of drillstring torsional vibration using LQR and fuzzy logic*', Journal of Petroleum Science and Engineering, Vol. 122, pp. 313–320, 2014.

[6] A.S. Sadiq, M.M. Khan, S.A. Shah and M. Jamil, '*A machine learning-based control framework for drilling automation*', Journal of Petroleum Science and Engineering, Vol. 207, 2021.

[7] B. Niu, D. He, Z. Xu and X. Wang, '*Intelligent stick-slip vibration control based on reinforcement learning*', IEEE Transactions on Industrial Informatics, Vol. 16, No. 9, pp. 6194–6202, 2020.

[8] J.J. Bailey and I. Finnie, '*An analytical study of drill-string vibration*', Journal of Engineering for Industry, Vol. 82, No. 2, pp. 107–114, 1960.

[9] Z. Tang and S. He, '*Nonlinear dynamic modeling and analysis of a drill string system*', Journal of Petroleum Science and Engineering, Vol. 67, No. 1–2, pp. 1–7, 2009.

[10] Y. Wang, Z. Chen, X. Liu and Y. Luo, '*Adaptive fuzzy neural control for uncertain nonlinear systems*', IEEE Transactions on Fuzzy Systems, Vol. 26, No. 2, pp. 673–685, 2018.

[11] Q. Bai and Y. Bai, '*Subsea Engineering Handbook'*, Gulf Professional Publishing, 2018.

[12] R. Temple, '*The Genius of China: 3,000 Years of Science, Discovery, and Invention*', Simon & Schuster, New York, USA 1986.

[13] --, '*Manual Percussion Drilling*', Akvopedia Website, Available at: https://akvopedia.org/wiki/Manual_percussion_drilling.

[14] J. C. Cumming, '*The Salt Industry of Central New York'*, Self-published, 1959.

[15] --, '*Spring Pole Drilling*', Engineering and Technology Wiki, Available at: https://ethw.org/Spring_Poles.

[16] D. Yergin, '*The Prize: The Epic Quest for Oil, Money, and Power'*, Simon & Schuster, New York, USA, 1991.

[17] J. Neshat, '*An Introduction to Rig Components*', ResearchGate. Available at: https://www.researchgate.net/publication/334964493_An_Introduction_to_Rig_Components.

[18] W. Rintoul, '*Spindletop*', Eakin Press, Austin - Texas, USA 1990.

[19] --, '*1866 Patent Rotary Rig*', American Oil and Gas Historical Society, Available at: https://aoghs.org/technology/1866-patent-rotary-rig.

[20] W. C. Goins and R. Sheffield, '*Blowout Prevention*', Gulf Publishing Company, Houston - Texas, USA 1983.

[21] P. Ramirez., '*Reserve Pit Management: Risks to Migratory Birds*', U.S. Fish and Wildlife Service Research Report, 2015, Available at: https://www.researchgate.net/publication/280946626_Reserve_Pit_Management_Risks_to_Migratory_Birds

[22] G. Boyadjieff, '*The Top Drive – A New System for Drilling*', in *SPE California Regional Meeting,* Paper SPE-13460-MS, 1985.

[23] --, 'Top Drive Systems', Lake Petro, Available at: https://www.lakepetro.com/top-drive.

[24] --, '*MWD: Measurement While Drilling'*, Sperry-Sun Publication, 1980.

[25] M. E. Cobern and E. B. Nuckols, '*Application of MWD Tools in Different Drilling',* 26th Annual Logging Symposium, Dallas - Texas, USA 1985.

[26] --, '*EM-MWD*', Native Navigation, Available at: https://nativenavigation.com/EM-MWD.

[27] M. W. Radler and H. Tang, *'Rotary Steerable Systems: A Decade of Innovation and Application*' in *SPE/IADC* Drilling Conference, Paper SPE-67751-MS, 2001.

[28] --, '*Attitude Control System for Directional Drilling Bottom Hole Assemblies*," ResearchGate, Available at: https://www.researchgate.net/publication/255521005.

[29] G. C. Lee, '*Offshore Structures Engineering'*, Gulf Publishing Company, Houston - Texas, USA 1981.

[30] --, '*Offshore Oil Platform*', Wikipedia, Available at: https://en.wikipedia.org/wiki/Offshore_oil_platform.

[31] --, '*The Rise of the Automated Rig*', Journal of Petroleum Technology, Vol. 73, No. 1, 2021. Available at: https://jpt.spe.org/a-robot-takes-over-the-drilling-floor.

[32] J. N. Reddy, '*An Introduction to the Finite Element Method'*, McGraw-Hill Education, New York, USA 2019.

[33] M. Khaled, E. Akkuratov, and C. Teodoriu, '*Development of a Simplified Transient Model for Real-Time Drilling Torque and Drag Simulations*'.

[34] M. B. Rubin, '*Cosserat Theories: Shells, Rods and Points'*, Kluwer Academic Publishers, Dordrecht, Netherlands 2000.

[35] E. Detournay and P. Defourny, *'A Phenomenological Model for the Drilling Action of Drag Bits*' *International Journal of Rock Mechanics Mining Science & Geomechanics Abstracts*, Vol. 29, No. 1, pp, 1992.

[36] J. B. Roberts and P. D. Spanos, '*Random Vibration and Statistical Linearization'*, Dover Publications, New York, USA 2003.

[37] Y. A. Khulief and F. A. Al-Sulaiman, '*Finite Element Dynamic Modeling of Drillstrings*', Finite Elements in Analysis and Design, Vol. 43, No. 13, pp. 987–1000, 2007.

[38] Z. Tariq, A. Abdulraheem, M. Mahmoud, T. Al-Ghamdi, and S. Elkatatny, *'Real-Time Drilling Operations Optimization Using Artificial Intelligence: A Systematic Review*' Journal of Petroleum Science and Engineering, Vol. 205, 2021.

[39] O. Bello, J. Holzmann, T. Yaqoob, and C. Teodoriu, '*Application of Artificial Intelligence Methods in Drilling System Design and Operations: A Review of the State of the Art*', Journal of Artificial Intelligence and Soft Computing, DOI: http://dx.doi.org/10.1515/jaiscr-2015-0024

[40] B. Elahifar, and E. Hosseini, '*A New Approach for Real-Time Prediction of Stick-Slip Vibrations Enhancement Using Model Agnostic and Supervised Machine Learning*', Journal of Petroleum Exploration and Production Technology, Vol. 14, pp. 175:201, 2023.

[41] S. Thomson and S. Mathur, '*Stick-Slip Vibrations Control Strategy Design for Smart Rotary Drilling Systems'*, in ICAIRES-2020 Proceedings, Springer, pp. 197–209.

[42] C. Wang, W. Chen, Z. Wu, J. Li and G. Liu, '*Stick–Slip Characteristics of Drill Strings and the Related Drilling Parameters Optimization*', Processes, Vol. 11, No. 9, 2023, DOI: https://doi.org/10.3390/pr11092783.

[43] M. Derbal, M. Gharib, S.S. Refaat, A. Palazzolo and S. Sassi, '*Fractional-Order Controllers for Stick-Slip Vibration Mitigation in Oil Well Drill-Strings*' Journal of Systems. Control Engineers, Vol. 235, No. 4, pp. 487–500, 2021.

[44] B. Talbi, A. Laib, and M. Gharib, '*Stick-Slip Stabilization in Oil Well Drill-Strings via Optimal Hybrid Fractional Order Fuzzy Logic Control Scheme*' Journal of Systems. Control Engineers, Vol. 237, No. 1, pp. 3–16, 2023.

[45] R. Riane, M. Z. Doghmane, M. Kidouche, K.F. Tee, and S. Djezzar, '*Stick-Slip Vibration Suppression in Drill String Using Observer-Based LQG Controller*', Sensors, Vol. 22, No. 16, 2023.

[46] Y. Jiang, K. Zhu, Q. Zhang, and S. Zhao, '*Stick Slip Vibration Control of Drill String Based on Torque Feedforward and Sliding Mode Controller*', Frontiers in Computing and Intelligent Systems, Vol. 3, No. 3, pp. 7989, 2021.

[47] Y. Jiang and Q. Zhang, '*Stick–Slip Suppression in Drill String Systems Using a Novel Adaptive Sliding Mode Control Approach'*, Sensors, Vol. 20, No. 2, 2020.

[48] J. Cheng, M. Wu, and L. Chen, '*Observer-Based Tracking Control for Suppressing Stick-Slip Vibration of Drillstring System*', In Proceedings of the 37th Chinese Control Conference, pp. 10254–10258, Wuhan, China 2018.

[49] A. Laib, B. Talbi, A. Krama, and M. Gharib, '*Hybrid Interval Type-2 Fuzzy PID+I Controller for a Multi-DOF Oilwell Drill-String System*,' IEEE Access, Vol. 10, pp. 67262 – 67275, DOI: https://doi.org/10.1109/ACCESS.2022.3185021

[50] W. Lin, J. P. Chavez, Y. Liu, Y. Yang and Y. Kuang, '*Stick-Slip Suppression and Speed Tuning for a Drill-String System via Proportional-Derivative Control*', Applied Mathematical Modeling, Vol. 82, pp. 487–502, 2020.

[51] B. D. O. Anderson and J. B. Moore, '*Optimal Control: Linear Quadratic Methods*', Prentice Hall, Englewood Cliffs, NJ, USA, 1990.

[52] C. Zang, Z. Lu, S. Ye, X. Xu, C. Xi, X. Song, Y. Guo and T. Pan, '*Drilling Parameters Optimization for Horizontal Wells Based on a Multiobjective Genetic Algorithm*', Applied Sciences, Vol. 12, No. 22, 2022.

[53] L. Mokrani, '*Intelligence Artificial Techniques*', Course Handout, Electrical Engineering Department, Laghouat University.

[54] I. E. Livieris and P. Pintelas, '*A Survey on Algorithms for Training Artificial Neural Networks*', University of Patras, Departmet of Mathematics, Technical Report TR08-01, Sep. 2008.

[55] Goodfellow, Y. Bengio, and A. Courville, '*Deep Learning*', MIT Press, Cambridge - MA, USA 2016. Available at: https://www.deeplearningbook.org/